

UNCLASSIFIED

1

AD-A206 730 INFORMATION PAGE

Form Approved
OMB No. 0704-0188

2a. SECURITY CLASSIFICATION AUTHORITY SECRET APR 12 1989		1b. RESTRICTIVE MARKINGS	
2b. DECLASSIFICATION / DOWNGRADING SCHEDULE		3. DISTRIBUTION / AVAILABILITY OF REPORT Approved for public release: Distribution unlimited	
4. PERFORMING ORGANIZATION REPORT NUMBER(S) H C 2		5. MONITORING ORGANIZATION REPORT NUMBER(S) AFOSR-TR-89-0388	
6a. NAME OF PERFORMING ORGANIZATION The Johns Hopkins University Applied Physics Laboratory	6b. OFFICE SYMBOL (if applicable)	7a. NAME OF MONITORING ORGANIZATION AFOSR/NC	
6c. ADDRESS (City, State, and ZIP Code) Johns Hopkins Road Laurel, Maryland 20707-6099		7b. ADDRESS (City, State, and ZIP Code) Building 410 Bolling AFB, DC 20332-6448	
8a. NAME OF FUNDING / SPONSORING ORGANIZATION AFOSR	8b. OFFICE SYMBOL (if applicable) NC	9. PROCUREMENT INSTRUMENT IDENTIFICATION NUMBER 400039-87-C-5381 AFOSR 85-0169	
8c. ADDRESS (City, State, and ZIP Code) 717 Architect Building 1400 Wilson Blvd. Arlington, VA 22209		10. SOURCE OF FUNDING NUMBERS	
		PROGRAM ELEMENT NO. 61102F	PROJECT NO. 2303
		TASK NO. A3	WORK UNIT ACCESSION NO.
11. TITLE (Include Security Classification) Final Report: Organo-metallic Elements for Associative Information Processing			
12. PERSONAL AUTHOR(S) Potember, Richard S. and Poehler, Theodore O.			
13a. TYPE OF REPORT Final	13b. TIME COVERED FROM 85/4/15 TO 88/4/15	14. DATE OF REPORT (Year, Month, Day) 89/1/15	15. PAGE COUNT
16. SUPPLEMENTARY NOTATION			
17. COSATI CODES		18. SUBJECT TERMS (Continue on reverse if necessary and identify by block number)	
FIELD	GROUP	Nonlinear optics, charge-transfer complexes, TCNQ, VO ₂ , conducting polymers, organic solids, neural networks, electrical switches, organic semiconductors, photochromics	
19. ABSTRACT (Continue on reverse if necessary and identify by block number)			
<p>In the three years of the program we have: (1) built and tested a 4 bit element matrix device for possible use in high density content-addressable memories systems; (2) established a test and evaluation laboratory to examine optical materials for nonlinear effects, saturable absorption, harmonic generation and photochromism; (3) successfully designed, constructed and operated a codeposition processing system that enables organic materials to be deposited on a variety of substrates to produce optical grade coatings and films. This system is also compatible with other traditional microelectronic techniques; (4) used the sol-gel process with colloidal AgTCNQ to fabricate high speed photochromic switches; (5) developed and applied for patent coverage to make VO₂ optical switching materials via the sol-gel processing using vanadium (IV) alkoxide compounds; (6) synthesized several compounds including TCNQ(N₂S)₂, for the study of bistable optical and optoelectronic switching under laser irradiation, and; (7) explored the possibility of using the excited state nonlinear properties of dyes and polymers for optical information processing applications.</p>			
20. DISTRIBUTION / AVAILABILITY OF ABSTRACT <input type="checkbox"/> UNCLASSIFIED/UNLIMITED <input checked="" type="checkbox"/> SAME AS RPT <input type="checkbox"/> DTIC USERS		21. ABSTRACT SECURITY CLASSIFICATION UNCLASSIFIED	
22a. NAME OF RESPONSIBLE INDIVIDUAL T. O. Poehler or R. S. Potember - Dr Ulrich		22b. TELEPHONE (Include Area Code) 301-953-6254/953-6251	22c. OFFICE SYMBOL NC

D Form 1473, JUN 86

Previous editions are obsolete.

SECURITY CLASSIFICATION OF THIS PAGE

89

UNCLASSIFIED

FINAL REPORT

1. TITLE: ORGANO-METALLIC ELEMENTS FOR ASSOCIATIVE INFORMATION PROCESSING

2. PRINCIPAL INVESTIGATOR: Dr. Theodore O. Poehler and
Dr. Richard S. Potember
The Johns Hopkins University
Applied Physics Laboratory
Laurel, Maryland 20707

3. INCLUSIVE DATES: 15 April 1985 - 15 April 1988

4. GRANT NUMBER: N00039-87-C-5301

5. COSTS AND FY SOURCE: (FY85/88)

6. SENIOR RESEARCH PERSONNEL: Dr. A. A. Burk, Dr. S-W. Hu

7. JUNIOR RESEARCH PERSONNEL: K. R. Speck, C. A. Viands, R. A. Murphy,
J. Curry, R. C. Hoffman, and J. E. Cocchiaro

8. PUBLICATIONS:

R. S. Potember, T. O. Poehler, R. C. Hoffman, K. R. Speck, and R. C. Benson, "Reversible Electric Field Induced Bistability in Carbon Based Radical-Ion Semiconducting Complexes: A Model System for Molecular Information Processing and Storage," 2nd International Workshop on Molecular Electronic Devices, edited by F. L. Carter, (Marcel Dekker, Inc., NY) 1985.

R. S. Potember, R. C. Hoffman, and T. O. Poehler, "Molecular Electronics," Johns Hopkins Technical Digest, April-June 1986, Vol. 7, No. 2.

R. C. Hoffman, T. O. Poehler, and R. S. Potember, "Characterization of an Erasable Organometallic Optical Storage Medium," Digest of Technical Papers, CLEO, 9-13 June 1986.

R. S. Potember, R. C. Hoffman, H. S-W. Hu, J. E. Cocchiaro, C. A. Viands, R. A. Murphy, and T. O. Poehler, "Electronic Devices from Conducting Organic Polymers," Polymer, Vol. 28, p. 574 (1987).

R. S. Potember, T. O. Poehler, K. R. Speck, R. C. Hoffman, and C. A. Viands, "Bistable Optical Threshold Switching in Organic Photochromic Materials," Bull. Am. Phys. Soc., Vol. 31, p. 657 (1986).

R. S. Potember, K. R. Speck, and H. S-W. Hu, "VO₂ Films Formed by the Sol Gel Process from Vanadium (IV) Tetraalkoxyl Compounds," Patent Disclosure, The Johns Hopkins University, March 1987.

R. S. Potember, R. C. Hoffman, H. S-W. Hu, and K. R. Speck, "Molecular Devices for Optical Computing," to appear in the 3rd International Workshop on Molecular Electronic Devices, ed. Forrest L. Carter (Elsevier, North-Holland) pp. 663-677 (1988).

R. S. Potember, R. C. Hoffman, H. S-W. Hu, J. E. Cocchiaro, C. A. Viands, and T. O. Poehler, "Electronic Devices from Conducting Organics and Polymers," *Polymer Journal*, Vol. 19, No. 1, pp. 147-156 (1987).

K. R. Speck, T. O. Poehler, and R. S. Potember, "Bistable Optical Switching in Organometallic Doped Gel Derived Silica Glasses," *The Fifth International Congress on Applications of Lasers and Electro-optics* (1986).

R. S. Potember, R. C. Hoffman, K. A. Stetyick, and R. A. Murphy, "Optical Threshold Elements Based on the Excited State Photophysical Properties of Molecular Materials," *Nonlinear Optical Properties of Polymers*, Editors A. J. Huger, J. Orenstein, D. R. Ulrich, *Materials Research Society Symposium Proceedings*, 109, 29-34, 1987.

R. S. Potember, R. C. Hoffman, S. H. Kim, K. R. Speck, and K. A. Stetyick, "Molecular Optical devices," *J. Molecular Electronics*, 4, 5 (1988).

K. R. Speck, H. S-W. Hu, R. A. Murphy, and R. S. Potember, "Vanadium Dioxide Films Grown from Vanadium Tetrakis(t-Butoxide) by the Sol-Gel Process," *Better Ceramics Through Chemistry III*, Editors C. J. Brinker, D. E. Clark, and D. R. Ulrich, 121, 667-672 (1988).

K. R. Speck, H. S-W. Hu, M. E. Sherwin, R. S. Potember, "Vanadium Dioxide Films Grown from Vanadium Tetraisopropoxide by the Sol-Gel Process," *Thin Solid Films*, 165, 317-322 (1988).

R. C. Hoffman and R. S. Potember, "Organometallic Materials for Erasable Optical Storage," accepted for publication by *Applied Optics*.

R. S. Potember, R. C. Hoffman, K. A. Stetyick, R. A. Murphy, and K. R. Speck, "Molecular Materials for Nonlinear Optics," *Johns Hopkins APL Technical Digest*, Vol. 9, No. 3, p. 189 (1988).

CONFERENCES

"Bistable Threshold Switching in Organic Photochromic Materials," presented at the American Physical Society meeting, Las Vegas, Nevada, 30 March-April 4, 1986.

"Bistable Threshold Switching in Organic Materials," R. S. Potember, T. O. Poehler, K. R. Speck, R. C. Hoffman, and C. A. Viands, presented at the Neural Networks for Computing Conference, Snowbird, Utah, 13-16 April 1986.

"Electronic Devices from Conducting Polymers," presented at 2nd International Polymer Conference, Tokyo, Japan, August 21, 1986.

"Bistable Optical Switching in Organometallic Doped Gel-Derived Silica Glasses," K. R. Speck, T. O. Poehler, and R. S. Potember, *The Fifth International Congress on Applications of Lasers and Electro-optics*, Arlington, VA, 10-13 November 1986

Distribution/Availability Codes	
Dist	Avail and/or Special
A-1	

"Electronic Devices from Conductive Organics," R. S. Potember, presented at Speciality Polymers '86, 6-8 August 1986, The Johns Hopkins University, Baltimore, MD.

R. S. Potember "Optical Threshold Materials for Symbolic Computing," AFOSR/DARPA Program Review, February 1987, Leesburg, VA.

R. S. Potember, "Molecular Optical Devices," Japan National Science Foundation Forum, Frontiers in Material Science, January 1987, Hakone, Japan.

R. S. Potember, "Molecular Devices for Optical Computing," Symposium on Molecular Electronic Devices, October 1986, Arlington, VA.

Invited speaker Symposium of Molecular Electronics and Biocomputers, "Molecular Optical Devices," Budapest, Hungary, 24-27 August 1987.

Invited speaker, National Academy of Science, National Research Council, "Opportunities in Molecular Materials," Washington, D.C., October 1987.

Invited speaker, Riken Institute, Japan, "Nonlinear Materials for Optical Computers," and "Sol-Gel Processing of VO₂ Thin Films," October 1988.

Invited speaker, Polymer Society Japan, "Optical Threshold Devices," Fukurka, Japan, October 1988.

9. ABSTRACT OF OBJECTIVES:

OBJECTIVES

The objectives of the program were (1) to investigate the optical switching characteristics of organic thin films that exhibit reversible phase transitions, (2) to use these materials as a basis for a new class of devices for use in optical information processing, and (3) to use these materials as a basis for a new class of devices for use in high density content-addressable memories and associative processors.

TABLE OF CONTENTS

I.	EXECUTIVE SUMMARY.....	I-1
II.	TEST AND EVALUATION OF MATERIALS FOR OPTICAL INFORMATION PROCESSING AND NONLINEAR OPTICS.....	II-1
III.	NOVEL CODEPOSITION PROCESSING OF ORGANOMETALLIC ELEMENTS.....	III-1
IV.	MOLECULAR DEVICES FOR OPTICAL COMPUTING.....	IV-1
V.	SYNTHESIS OF NOVEL MATERIALS FOR LARGE SCALE ELECTRICAL AND OPTICAL NETWORKS.....	V-1
	A. Progress Section.....	V-1
	B. Experimental Section.....	V-9
VI.	TWO TERMINAL ORGANOMETALLIC LOGIC ELEMENT FOR NOVEL COMPUTER ARCHITECTURE APPLICATIONS.....	VI-1
VII.	SOL-GEL GLASSES FOR OPTICAL INFORMATION PROCESSING MATRICES.....	VII-1
VIII.	VO ₂ FILMS BY THE SOL-GEL PROCESS	VIII-1

10. ACCOMPLISHMENTS

I. EXECUTIVE SUMMARY

We have taken an aggressive approach at The Johns Hopkins University Applied Physics Laboratory to apply molecular solids to several novel optical and electrical information processing and storage applications.

In the three years of the program we have: (1) built and tested a 4 bit element matrix device for possible use in high density content-addressable memories systems; (2) established a test and evaluation laboratory to examine optical materials for nonlinear effects, saturable absorption, harmonic generation and photochromism; (3) successfully designed, constructed and operated a codeposition processing system that enables organic materials to be deposited on a variety of substrates to produce optical grade coatings and films. This system is also compatible with other traditional microelectronic techniques; (4) used the sol-gel process with colloidal AgTCNQ to fabricate high speed photochromic switches; (5) developed and applied for patent coverage to make VO₂ optical switching materials via the sol-gel processing using vanadium (IV) alkoxide compounds; (6) synthesized several compounds including TCNQ(N₂S)₂, for the study of bistable optical and optoelectronic switching under laser irradiation, and; (7) explored the possibility of using the excited state nonlinear properties of dyes and polymers for optical information processing applications.

This final report discusses each of the above technical areas in further depth and provides a summary of our three year program.

II. TEST AND EVALUATION OF MATERIALS FOR OPTICAL INFORMATION PROCESSING AND NONLINEAR OPTICS

Introduction

Recent advances in optical characterization capabilities pertinent to the advanced optical materials produced at APL are described. Properties of interest in advanced optical materials include but are not limited to; nonlinear effects such as saturable absorption and harmonic generation, and photochromism or any other optical change which can be exploited for optical information processing. Listed below are several optical characteristics which may serve as optical processing mechanisms. There are at least five potential mechanisms we have explored for achieving this goal.

<u>Mechanism</u>	<u>Effect on Transmitted Light</u>
1. Variable optical absorption	reduce intensity
2. Variable optical reflection	reduce intensity
3. Variable optical rotation	change polarization
4. Variable optical phase shifting	change phase
5. Variable optical refraction	change angle of propagation

Our efforts concentrated on finding materials exhibiting these mechanisms to evaluate their speed and magnitude to determine the most promising systems for future experimentation.

Experimental

Figures 1 - 4 contain examples of the experiments which can be performed in the optics test and evaluations laboratory. These experiments include measurement of nonlinear, -transmission, -reflection, -emission, harmonic generation, optical rotation, and self focusing-defocusing. Transmission as

referred to here can be reduced by both reflective, scattered and absorptive losses. The independent measurement of reflection allows separation of reflective and absorptive losses given negligible scattering. The basic measurements of transmission and reflection in Figure 1 are readily modified, with the incorporation of selective bandpass filters, to the measurement of emission and harmonic generation in Figure 2. The incorporation of polarizers in Figure 3 allows observation of optical rotation of plane polarized light resulting from the optically induced Kerr effect and/or any non-linear optical activity. The observation of self focusing-defocusing requires more elaborate optics as shown in Figure 4. These focusing effects are manifestations of nonlinear indices of refraction and can be complicated by accompanying nonlinear reflection or absorption.

In addition to the single wavelength experiments mentioned above the capability exists to generate the 1st harmonic and then use it to modulate the optical properties of the material under study at the fundamental wavelength as shown in Figure 5. For example, a saturable absorber at $0.53 \mu\text{m}$, with a higher absorption cross section in the electronic excited state than ground state for $1.06 \mu\text{m}$ light would have nonlinear absorption at $1.06 \mu\text{m}$.

Two types of detectors are employed in all the above experiments: average powers measured by Scientech calorimeters result in plots of optical excitation power vs. response (transmission, reflection, etc.) on a x-y recorder; Ge photodiodes are used with an oscilloscope to monitor temporal pulse shape with approximately 1-2 nanosecond resolution. This allows for a measure of the speed of nonlinear effects.

Results and Discussion

In this section experimental results obtained with the new optical equipment are presented and discussed. One of the following results is a

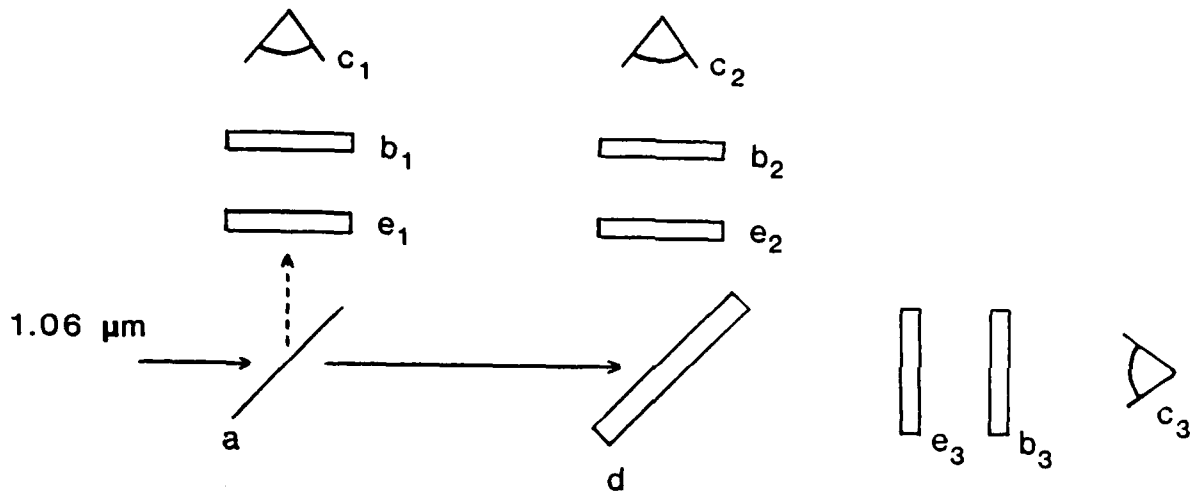


Fig. 1 Apparatus for measuring nonlinear transmission and reflection: a) beamsplitter; b) 1.06 μm interference filters; c) photodetectors; d) sample; e) neutral density filters.

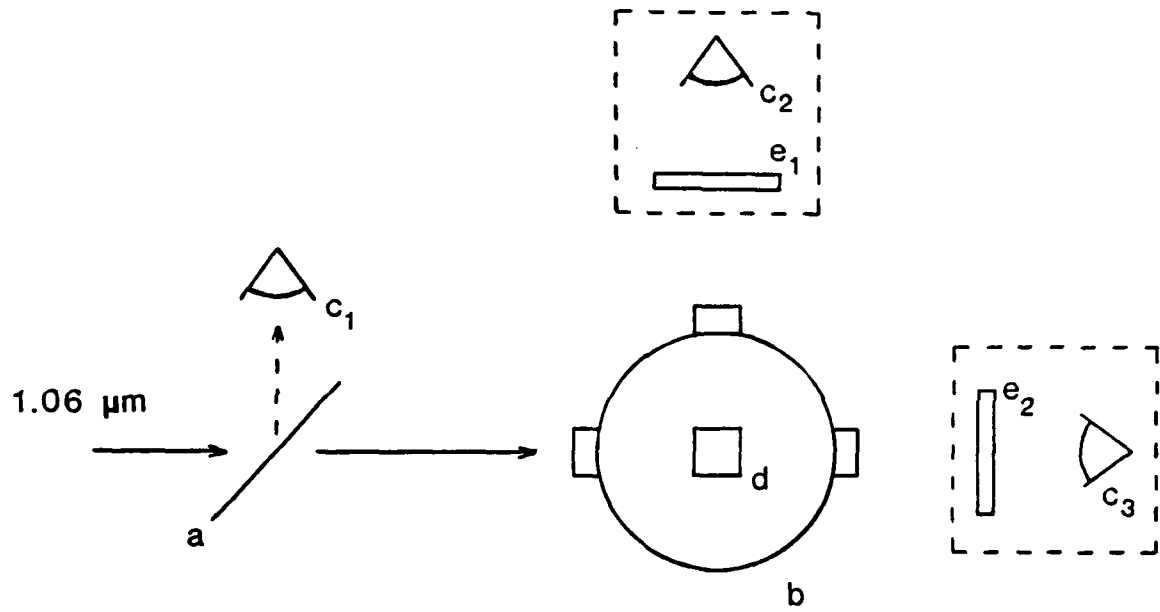


Fig. 2 Apparatus for measuring nonlinear emission and harmonic generation: a) beamsplitter; b) integrating sphere; c) photodetectors; d) sample; e) 1.06 μm blocking filters; dashed boxes -- optional positions.

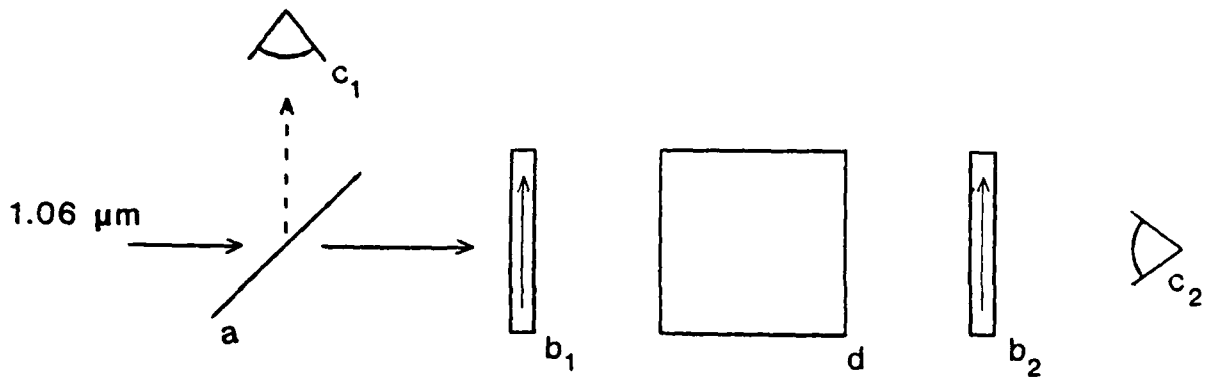


Fig. 3 Apparatus for measuring optical rotation: a) beamsplitter; b) polarizers; c) photodetectors; d) sample.

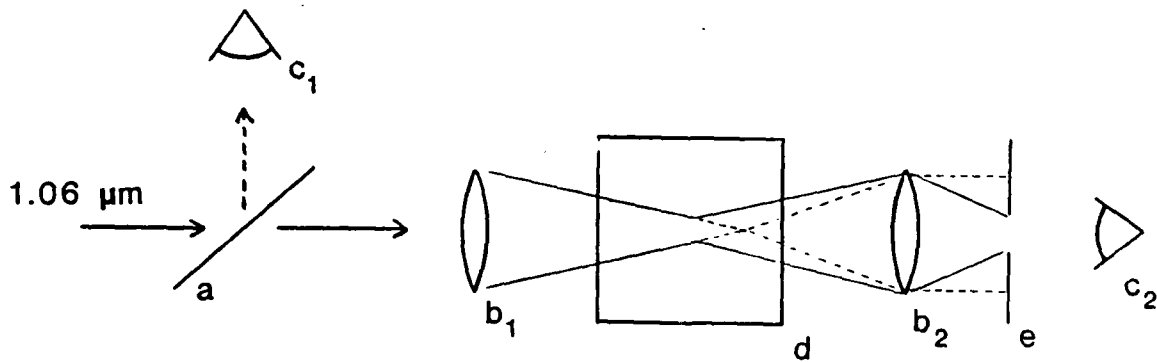


Fig. 4 Apparatus for measuring self focusing-defocusing: a) beamsplitter; b) lenses; c) photodetectors; d) sample; e) pinhole; solid line -- low light intensity path; dashed line -- high light intensity path; (adapted from M. J. Soileau, W. E. Williams, E. W. VanStryland, IEEE J. of Quantum Elec. QE-19 (4), 731 (1983)).

reproduction of a literature study for the purpose of familiarization with and calibration of the new optical set-up; the rest are original observations of novel metal-TCNQ optical switching properties.

CuTCNQ -

Data on CuTCNQ optical switching are now presented. CuTCNQ was chosen over AgTCNQ for these initial studies as earlier work in the group suggested a larger change in absorption, upon switching, at $1.06 \mu\text{m}$ for the Cu salt. The CuTCNQ films were made in the conventional manner; 200 \AA thick Cu films were coated with TCNQ and then reacted on a $240 \text{ }^\circ\text{C}$ hotplate.

A yellow irregularly shaped spot forms on the CuTCNQ film upon irradiation with approximately 50 mW average power ($1.06 \mu\text{m}$, 10 Hz Rep Rate) as measured by a Scientech power meter. Simultaneous single optical pulse (above optical threshold) monitoring of a reference and transmitted pulse with Ge-photodiodes, showed no observable change in temporal peak shape. This observation may result from the change in transmission at $1.06 \mu\text{m}$ being too small, fast or slow to be detected with our current set-up.

In another experiment, as the increase in transmission is large upon complete ablation of the CuTCNQ film, the transmission at $1.06 \mu\text{m}$ was monitored in real time during a single pulse of sufficient intensity to remove the film. In this extreme case the oscilloscope traces indicate a marked increase in transmission within 5-10 ns of the pulse leading edge.

In another related experiment, transmission of 632.8 nm light was monitored as a function of the number of $1.06 \mu\text{m}$ light pulses. After each $1.06 \mu\text{m}$ pulse the transmitted power of a 632.8 nm probe beam was observed to increase as shown in Figure 6. When the intensity of the $1.06 \mu\text{m}$ beam was adjusted to be just above optical threshold it took many pulses (over 30) to reach a limiting transmission.

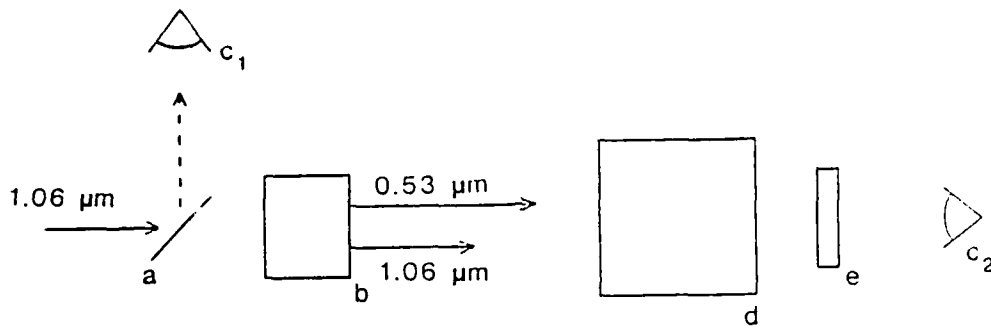


Fig. 5 Apparatus for measuring dual-wavelength effects: a) beam splitter; b) frequency doubler; c) photodetectors; d) sample; e) 0.53 μm blocking filter.

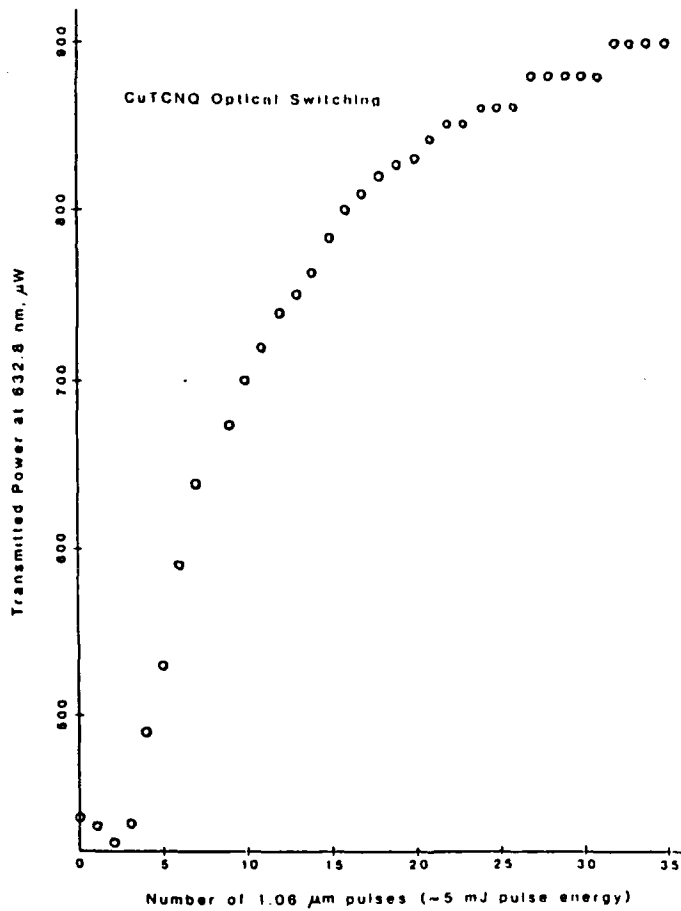


Fig. 6 Transmitted power at 632.8 nm through CuTCNQ as a function of the number of 1.06 μm pulses

Although the transmission change at 632.8 nm between any two pulses is not large, an attempt was made at monitoring this change real-time with a Ge-photodiode. The initial oscilloscope traces indicate that the transmission increase induced by the 1.06 μm light pulse is not completed during the 10 nanosecond pulse but instead may require 10's of nanoseconds or more for completion. Second year efforts with real-time measurements included several experimental modifications intended to improve the signal to noise ratio at 632.8 nm in order to more accurately determine the optical switching speed of CuTCNQ. These improvements included the incorporation of a fast amplifier (Comlinear model E104 (DC to 1.1 GHz bandpass), substitution of the Ge with a Si photodiode (twice the sensitivity at 632.8 nm), and the use of a more intense probe beam.

Average Power Measurements -

Simultaneous measurement of incident and transmitted optical power (1.06 μm , 10 Hz) is accomplished with two Scientech power meters and a recently completed BCD to analog converter circuit. In order to test the ability of the optical bridge to measure optical nonlinearity a sample of bis-(4-dimethylamino-dithiobenzil)-nickel (BDN), a known saturable absorber at 1.06 μm was studied.* The transmission of a 1×10^{-3} M solution of BDN in 1,2 dichloroethane is clearly nonlinear with excitation intensity as shown in Figure 7. This particular sample (1 cm pathlength) transmits approximately 12% at low light intensities (≤ 10 mW) and approximately 21% at 47 mW. This nonlinearity is reversible as evidenced by identical forward and reverse scans.

Optical transmission measurements on AgTCNQ and CuTCNQ are represented in Figure 8, as they both behave similarly. At low incident light intensities (< 30 - 40 mW) transmitted power is linear with increasing excitation power; $\approx 50\%$ T for the samples studied. At approximately 40-60 mW the transmission begins to

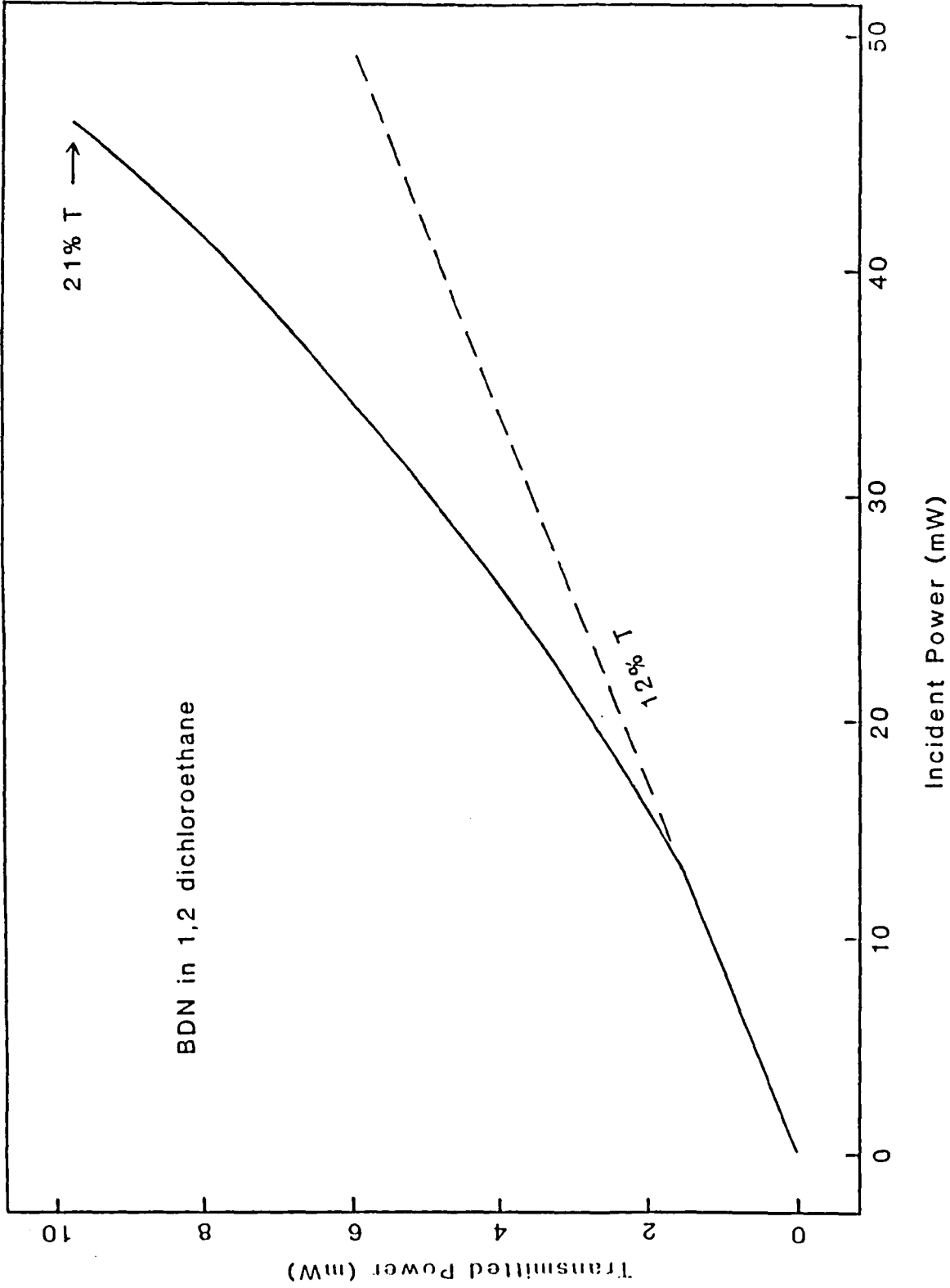


Fig. 7 Transmitted power at 1.06 μm through 1 cm of a 1×10^{-3} M solution of bis-(4-dimethylaminodithiobenzil)-nickel(BDN) in 1,2 dichloroethane as a function 1.06 μm incident power.

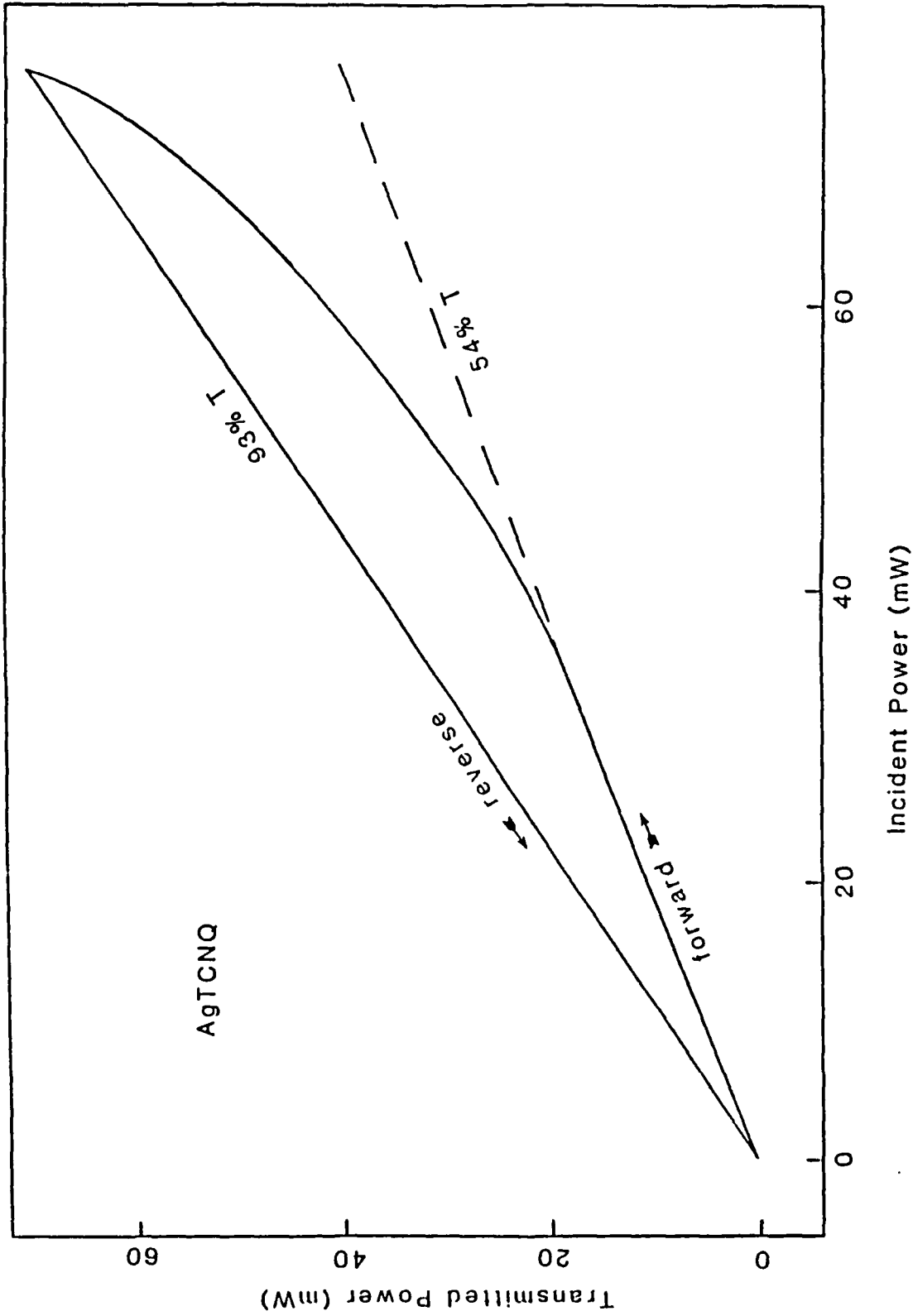


Fig. 8 Transmitted power at 1.06 μm through an AgTCNQ sample as a function of 1.06 μm incident power.

increase, corresponding roughly with the appearance of a yellow spot. The transmission continues to increase at higher excitation intensities and reaches approximately 90% T before film ablation is apparent. In the reverse scan, with decreasing excitation intensity the percent transmission remains constant resulting in a large hysteresis.

Additional metal TCNQ derivative salts were optically characterized, along with novel sol preparations of these salts in the search for new and valuable optical materials. These results are discussed elsewhere in this report.

Summary

This section has described recent developments in optical characterization capabilities pertinent to advanced optical materials produced at APL. These new capabilities allow for the search for optical processing and nonlinear optical materials. The ability to observe optical nonlinearity has been demonstrated with the dye BDN. Preliminary experiments performed on the novel metal-TCNQ charge-transfer salts have yielded valuable information on the optical transmission above and below optical threshold.

Experimental Capabilities

This section provides a general description of, and types of experiments performed in, our new optics test and evaluations laboratory:

Purpose - To characterize novel materials for potential use in optical information processing systems.

Physical Description - The facility occupies about 350 sq. ft. in the Milton S. Eisenhower Research Center. The laboratory centers around a vented 4' x 8' optical table and a Quantel Model 580-10 pulsed Nd:YAG laser.

Capabilities - The Optical Test and Evaluation Laboratory is capable of measuring nonlinear optical phenomena in materials including saturable and reverse-saturable absorption, photorefraction, emission saturation, and

harmonic generation. These behaviors can be measured on an average optical power and/or single pulse basis (1-2 nanosecond resolution).

Equipment - Major pieces of equipment in the laboratory include:

4' x 8' optical table

Quantel Model 580-10 Nd:YAG laser

Tektronix Model 7844 400 MHz oscilloscope

Hamamatsu Model B2297-3 Ge photodiodes

Sciencetech Model 365 power meter

Miscellaneous optical components (i.e., harmonic beam splitters, cutoff (long pass) filters, high energy laser polarizers and neutral density filters.

Miscellaneous electronic equipment (i.e., DC power supply, x-y chart recorder, pulse generator).

III. NOVEL CODEPOSITION PROCESSING OF ORGANOMETALLIC ELEMENTS

We have previously shown that organometallic charge-transfer complexes can be produced in a highly oriented thin film form by a solid-state diffusion process. Various metal-organic crystalline films are prepared by this solid-state diffusion process in a two-step procedure. First, the organic compound is vacuum deposited or sublimed onto a suitable metal substrate or transparent substrate supporting a thin metal film. In the second step, the complex is formed by heating which initiates a topotatic electron transfer reaction between the metal and organic layers. These high quality films exhibit enhanced optical properties. Scanning electron microscopy has revealed that these films are very uniform with a smooth featureless surface down to the micron level.

A new system for codeposition of donor metal and organic acceptor onto a substrate held at a carefully controlled temperature has been constructed and tested. The apparatus consists of a Veeco Model 776 vacuum station that has been refurbished and modified to meet our specific demands.

Using this system we are attempting to make metal-organic thin films that exhibit a lower switching threshold to optical irradiation than was observed when films were fabricated using stepwise deposition processes.

The codeposition process is performed by simultaneously depositing a metal (silver or copper) by evaporation and a neutral acceptor molecule by sublimation in single vacuum chamber. Careful control of the two deposition processes has produced metal organic thin films on a variety of substrates. These films are uniform in nature and provide increased control over the morphology of the resultant organic layer.

We have shown that the codeposition process and variations thereof allow great flexibility in organometallic (charge transfer) thin film fabrication.

Thus far, four basic synthetic techniques have been explored:

1. The donor metal is exposed to a molecular beam of organic acceptor while being held at an elevated temperature;
2. Alternating layers of metal and organic are deposited then heated either in vacuo or in an inert atmosphere (created by back-filling the vacuum chamber);
3. A layer of organic compound is deposited, followed by a layer of metal; and
4. Simultaneous deposition of metal and organic onto a substrate held at room temperature or above.

Each of the above techniques offers the advantage of complete processing in a fairly contaminant (mainly oxygen) free environment.

We have completed several successful experiments using this approach. CuTCNQ films of differing thickness (500-2000Å) have been produced by exposure of copper metal (on glass substrate) held at various temperatures to TCNQ vapor. Experiments are being performed in order to determine any thermodynamic (temperature), kinetic, and metal thickness restrictions and/or limitations.

Films have also been produced by depositing a thin layer of TCNQ followed by a thin layer of silver metal. The films appear non-stoichiometric possibly containing neutral TCNQ mixed into the organometallic structure. In this case, it is believed that the hot condensing metal vapor provides the required activation energy for the reaction. Further experimentation is underway to determine the composition, structure, and switching properties of these films and to attempt the fabrication of stoichiometric complexes using both copper and silver metals.

AgTCNQ films have been prepared by utilizing the codeposition of silver metal and TCNQ powder onto a substrate held at room temperature. This process is quite system-dependent particularly with respect to reactant evaporation rates and substrate positioning; thus, reproducibility is currently a problem. Minor design adjustments are being considered to overcome this obstacle, however. In addition, some films produced using this technique appear non-stoichiometric. Contrary to the previously described films, these may have a metal to TCNQ ratio of greater than one. Khatkale and Devlin (J. Chem. Phys. 70(04), 1851 (1979)) have reported the synthesis of the dianion (Na_2TCNQ) and trianion (Na_3TCNQ) salts of sodium TCNQ using a similar cocondensation method. Structural and optical characterization of the films is currently being performed. Due to the greater control of the organometallic thin film morphology and composition produced in this fashion, the codeposition technique will be emphasized in future work.

IV. MOLECULAR DEVICES FOR OPTICAL COMPUTING

A. All-Optic Logic Devices

All-optical devices are switches controlled by the incident intensity of the optical beam. Optically controlled switches are approximately 1000 times faster than corresponding electrically controlled devices making real time processing attainable. An advantage of all-optical devices is elimination of electromagnetic interference or crosstalk that often plagues electronic devices in tightly packed circuits.

There are two basic types of all-optical switching devices being proposed for digital optical computing. These two types of devices, the optical threshold device and the bistable optical device, can be classified by their functional application to information processing.

A plot of optical input power versus output power for idealized devices of both systems is shown in Figure 1. In Figure 1(a), the output power increases linearly as the input power is increased until a critical threshold value is reached. At this threshold point the output jumps sharply to a high output regime. As the input intensity is decreased, the optical input returns to the low output regime by the same path. The two linear regions of this "S" curve represent the two states of the optical device namely the "off" and "on" or "0" and "1" states. A single threshold device can perform signal amplification and the basic logic operations such as A/D conversion, AND and OR functions by simply selecting the appropriate incident beams supplied to it.

The optical characteristics of a bistable optical device, as shown in Figure 1(b), are similar to Fig. 1(a) because it can also exist in two stable states for a given set of input signals. However, the optical characteristics of the bistable optical device differ from that of the threshold device because on decreasing the input signal, the output does not immediately drop

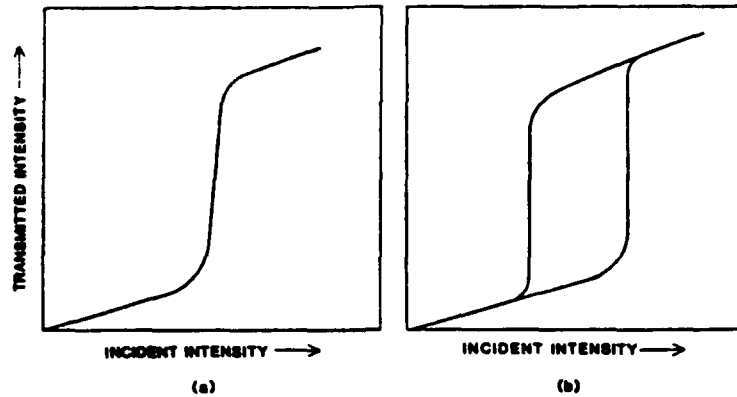


Fig. 1 Typical transmission of a bistable optical device.

to the low transmitting regime. This hysteretic loop can be used to add a short-term memory function to the operation of these bistable optical devices.

An optical transistor can be demonstrated in both types of all-optical devices by combining two optical beams in the nonlinear material to produce a single output beam. A schematic of an idealized all-optical transistor is shown in Figure 2. By adjusting the intensity of two input beams so that one input beam is close to, but not exceeding the threshold and a second much smaller signal is added to the first beam so that the materials threshold is exceeded, an optical output signal emerges. In this manner the weak beam is

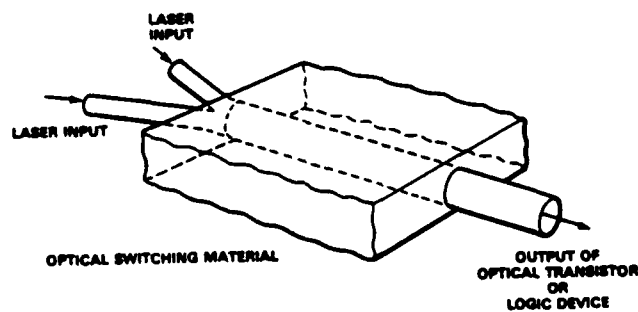


Fig. 2 Schematic of an optical switching device.

B. MATERIALS FOR PHOTONIC COMPUTING

1. Inorganic Semiconductors

The discovery of nonlinearities in narrow band gap semiconductors, (such as indium antimonide with a transition energy of 0.2 eV at 77 K), allowed for steady-state optical bistability to be demonstrated in a simple Fabry-Perot interferometer configuration [4]. Currently, well over twenty inorganic materials exist with reported intrinsic optical bistability. Other semiconductors with well characterized behavior are zinc selenide and zinc sulfide which showed room temperature nanosecond switching via a thermal mechanism in an interference filter arrangement using visible light at 514 nm [5]. Gallium arsenide etalons and GaAs-AlGaAs multiple quantum well structures, when inserted into a Fabry-Perot cavity, demonstrated subpicosecond ON and OFF switching times at an excitation wavelength of 827 nm [6].

Optical computing may be possible using inorganic semiconductors. They exhibit fast switching times (~1 ps), low device power consumption (~1 mW), and are thermally stable (up to 300 K). Yet, a major disadvantage of using these small band gap semiconductors is the limited transmission window often observed in these materials. This narrow transmission window prevents these materials from being used with many common laser sources.

2. The Advantages of Molecular Materials

Organic, biological and polymeric materials are being investigated for possible use in all-optical processing applications. A myriad of organic and polymeric materials exist with well characterized photophysical properties. Many organic materials, especially polymers because of their high degree of cross-linking, exhibit a greater resistance to laser damage than do ionic crystalline materials. In addition, many organics are more transparent than inorganic optical materials at certain frequencies, and the wavelength depend-

ence of transparency can be controlled by synthetic design to match specific laser frequencies. Finally, organic materials offer the promise of storing and processing information at the "molecular level." Recent reports of voltage-tunable optical data storage using persistent spectral hole burning [7] and reversible multiple-state optical recording using organic charge transfer complexes are a first step toward this realization [8].

3. Organic Photochromics

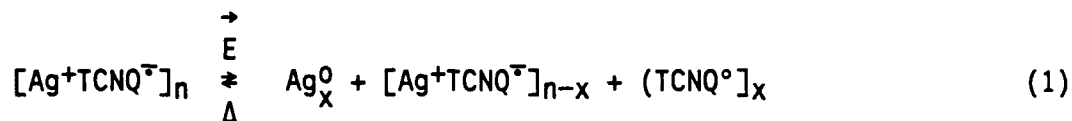
Organic compounds with discrete optical states are currently being explored for optical storage i.e., optical memories and processing. The reversible photochemical reaction in this class of materials can convert a single chemical structure between two stable isomers which often exhibit two distinct absorption maxima. Organic photochromic compounds such as spiroopyrans and aberchrome dyes are being developed for use in reversible optical memories. In addition to optical memories, these materials are being used for optical data processing, spatial light modulation and optical waveguide devices.

4. Bistable Switching Organometallics Materials in Gel-Derived Glasses

We have recently reported an all-optical bistable switching effect in a class of organic charge transfer complexes based on silver-TCNQ and its chemical derivatives [9-13]. When the organometallic complex was doped into a gel-derived silica glass, changes in the materials' absorption were used to demonstrate optical logic operations using moderately powered continuous or pulsed laser radiation at several wavelengths [14].

Bistable optical switching has been reported in the organometallic compound AgTCNQ when exposed to incident laser radiation above a characteristic threshold power level. It has been postulated that the effect of the applied optical field on the initial charge-transfer complex is to cause an electric field

induced phase transition resulting in the formation of a non-stoichiometric complex salt containing neutral TCNQ, as shown in Reaction (1)



The original charge-transfer complex can be reformed by heating the complex salt solid phase. Observed changes in the optical properties of AgTCNQ are a direct consequence of this electric field induced effect which breaks the weak ionic bond between the metal cation and the organic radical anion via an excited state electron transfer reaction. The reported switching time from the simple charge-transfer complex to the mixed complex containing neutral molecules is reported to be less than 4 nsec.

Silver-TCNQ was prepared in colloidal form, with particle sizes ranging from 0.22 to 2.50 microns, by the reaction of LiTCNQ and aqueous AgNO₃ according to the procedure described by Melby et al [15]. Gel-derived monolithic glass gate array processors containing AgTCNQ were prepared by hydrolyzing and polymerizing TMOS (tetramethyl orthosilicate). The gels were converted to glasses by heating at 60°C for one week. Typical gel-derived glass disks were 2.5 cm in diameter and 1 mm thick. The AgTCNQ remained uniformly dispersed during this transformation.

The optical absorption spectrum of a gel-derived glass containing dispersed AgTCNQ particles is shown in Figure 3. The absorption peaks have been identified and interpreted in previous reports on the optical spectra of powder TCNQ compounds in KBr pellets [16-17]. The same disk was then irradiated above threshold by a Nd:YAG laser operating at 1060 nm. The Nd:YAG laser was pulsed at a 10 Hz repetition rate with an average power of 600 mW. Upon irradiation, the dark blue color of the AgTCNQ rapidly transformed into a pale

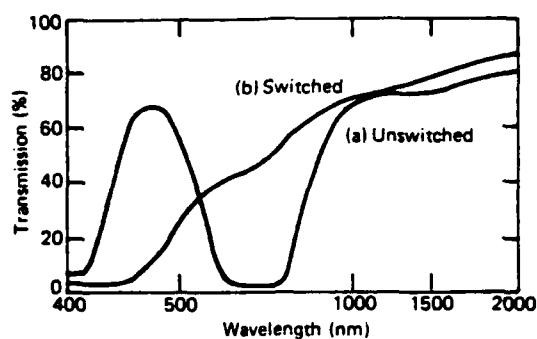


Fig. 3 Typical AgTCNQ transmission switch.

yellow color characteristic of the formation of neutral TCNQ, as indicated by the curve labeled (b) in Figure 3. This large change in transmission observed in these organometallic compounds incorporated in a glass matrix makes these nonlinear materials possible candidates for use in high speed optical logic devices.

The threshold nature of these gel-derived glasses containing AgTCNQ has been used to demonstrate A/D conversion and various logic operations. An all-optical logic device is shown schematically in Figure 4.

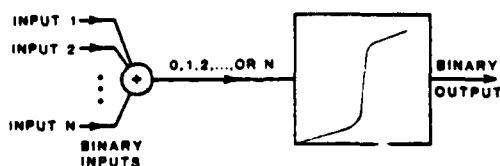


Fig. 4 N-input binary logic gate.

To demonstrate the threshold effect in these materials, samples were irradiated with various combinations of two laser beams and changes in the output transmission were monitored. Irradiation from one or more independent optical beam focused on one spot on the disk with a combined optical output below threshold results in no change in transmission. Proof of demonstration of

three all-optical logic operations with a temporary memory effect was performed using these organic bistable materials in a gel-derived glass gate array. An AND logic operation and optical transistor were demonstrated in concept by using two Nd:YAG laser beams (1060 nm), each of which is below the threshold power level for switching. When the sum of the two beams added together exceeded the threshold value for the organic complex, the irradiated area became transmitting, and an increase in the output signal was detected. By setting one optical input signal close to the optical threshold and by using a second much smaller input signal the concept of an optical transistor was shown, as discussed previously.

The materials have been made to perform as a logic OR gate. Irradiation from one or more independent optical beams focused on one spot on the disk with a single or combined optical output below threshold results in minimal transmission. However, increasing the intensity of either laser beam above the threshold results in the rapid increase in transmission.

By altering the wavelength of the Nd:YAG laser to a line (532 nm) that is less transmitting in the switched state than the unswitched state, an Exclusive OR (XOR) gate device was demonstrated. Below threshold, the AgTCNQ complex salt became more absorbing in the green spectral region and the measured output intensity decreases.

Work is continuing in this area to reduce the optical threshold of switching and to increase the cycling time of these materials. Currently the reversal of the switching process is limited by phase segregation of the donor and acceptor species, due to the large influx of thermal energy from the relatively long 10 nsec pulses. Pulses in the picosecond regime are more suitable as there is less of a thermal component. This problem must be addressed before large monolithic arrays of these optical switching devices can be used for optical computing.

5. Optical Threshold Elements Based on the Excited State Photophysical Properties of Molecular Materials

We have explored several classes of organic dye macromolecular systems to develop an all-optical "real time" threshold logic element based on their excited state photophysical properties. In order for a nonlinear material to find use in optical switching applications several criteria must be satisfied. These are summarized below.

- (i) Optically induced nonlinearity.
- (ii) Fast switching and recovery time.
- (iii) Stability to thermal and laser damage.
- (iv) Optical activity at common laser wavelengths.
- (v) Low optical threshold powers.
- (vi) Processability into device structures.

Table II shows a compilation of the basic photochemical events and processes common in organic molecules ranked in decreasing order of rate for the corresponding event to occur. In order for a photochemical process to be of interest for optical processing applications, the time scale of the event must be less than 10^{-9} seconds (subnanosecond). Applying this prerequisite to the search for novel materials and processes, one can observe from Table II that almost all chemical reactions involving the formation of an actual product are too slow to be considered for application to real time optical processing. The events that meet this prerequisite include dynamic events such as electronic motion, electron orbit hopping, electron or proton transfer, rotational and translational motion of small molecules, and bond cleavage.

We have explored molecular systems that use electron transitions to excited states to produce nonlinear optical phenomena. Specifically, we have investi-

gated the nonlinear absorption reported in many dye chromophores. In an organic dye chromophore, the absorption of visible light and subsequent electronic motions in the chromophores pi-electron system are on the order of 10^{-12} seconds.

Table II Time Scale of Molecular Processes

TIME SCALE (SEC)	PHOTOCHEMICAL EVENT	
fs	10^{-15}	ELECTRONIC MOTION ELECTRON ORBITAL JUMPS ELECTRON TRANSFER PROTON TRANSFER VIBRATIONAL MOTION
ps	10^{-12}	BOND CLEAVAGES (WEAK) ROTATION AND TRANSLATIONAL MOTION (SMALL MOLECULES, FLUID) BOND CLEAVAGES (STRONG) SPIN ORBIT COUPLING
ns	10^{-9}	ROTATIONAL AND TRANSLATIONAL MOTION (LARGE MOLECULES, FLUID) HYPERFINE COUPLING
μsec	10^{-6}	"ULTRAFAST" CHEMICAL REACTIONS
ms	10^{-3}	ROTATIONAL AND TRANSLATIONAL MOTION (LARGE MOLECULES AND/OR VERY VISCOUS)
—	10^0	"FAST" CHEMICAL REACTIONS
sec	10^2	
min	10^4	"SLOW" CHEMICAL REACTION

For certain classes of dye chromophores called saturable absorbers [18], the photo-induced excited state absorption cross section is lower than the ground state absorption cross section. The ground state absorption cross section is determined simply from the ratio of the incident and emerging monochromatic beams on a dye sample. This decrease in the excited state cross section results in a decrease in the absorption as the intensity of the incident radiation is increased to modest power levels. The mechanism for describing this theory is quite involved due to the complexity of organic

structures, but a Jablonski energy diagram can be used as a simple model to illustrate this effect.

Figure 5 shows an energy level diagram of an idealized saturable absorber. At low levels of optical intensity the optical transparency of the material does not change appreciably. As the incident radiation intensity increases, the population of the first excited state, S_1 , also increases. This is accompanied by nonradiative decay from these vibrationally excited states to the lowest vibrational manifold of the first excited state. The population of the ground state becomes depleted at moderate power levels (but below the level of laser damage). At these moderate power levels, the absorption coefficient of the saturable absorber begins to drop sharply and the material becomes increasingly transparent. At these higher intensities, the first excited state becomes highly populated, acting as a trap, and excitations from the first excited state to higher excited states, S_2 , begin to dominate the photo-physical behavior of the material. Under conditions where the absorption cross section of the ground state is greater than the absorption cross section of the first excited state, saturable absorption will occur. The material will remain in this highly transparent state as long as the metastable excited state remains heavily populated. Depopulation of this state is believed to be due to a complex relaxation mechanism.

A simplified example of saturable absorption can be seen in the coumarin chromophore derivatized with an amino group in the 7-position as shown in Figure 6. The electronic ground state, S_0 , has a π -electron distribution and an absorption spectrum closely resembling the mesomeric form A. Resonance structure B makes little contribution to the π -distribution. Upon optical excitation to the first excited singlet state, S_1 , the polar mesomer B is predominant and the absorption spectrum is characterized by a shift of the main

absorption band to longer wavelengths. In form B, the static electric dipole moment formed in the chromophore is stabilized by electron-donating alkyl groups on the relatively electropositive N atom and by conjugation.

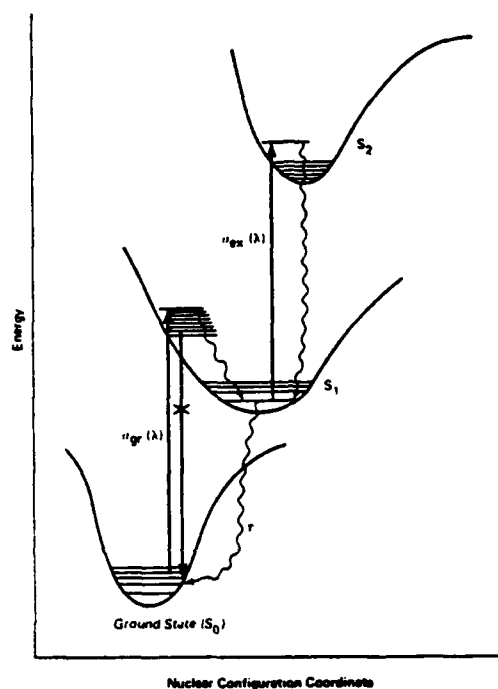


Fig. 5 Schematic of electronic energy levels of an idealized saturable absorber.

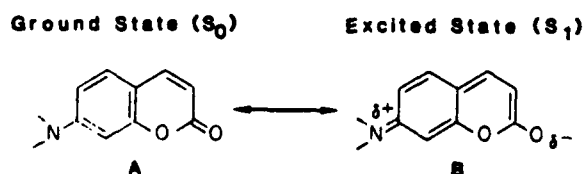


Fig. 6 Mesomeric forms of coumarin chromophore.

Although most saturable absorbers have been studied in a cell containing an organic solvent for Q-switching and stabilization of laser sources, we are

investigating the optical saturation of electronic transitions in organic molecules and polymers containing dye chromophores such as polymethine-pyrylium, -benzothiopyrylium and -thiapentacarbocyanines in thin film form, as single crystals and in a variety of solid matrixes.

6. Nonlinear Absorbers Based on the Indanthrone Chromophore

An example of an organic molecule exhibiting nonlinear behavior in its absorption that we have begun to investigate in depth is the indanthrone molecule, which was first synthesized in 1903 by Bohn from 1-amino-2-bromo-anthraquinone [19]. It has been known for some time that indanthrone exhibits the phenomenon of saturable transmission [20]. Saturable transmitters like indanthrone become more absorbing as the incident intensity increases, as opposed to the phenomenon of saturable absorption where the material becomes more transmitting as the incident intensity increases.

An aqueous solution of indanthrone ($4.5 \times 10^{-5} \text{M}$) exhibits an incident intensity versus transmitted intensity curve typical of a reverse saturable absorber, as shown in Figure 7. We obtained the preliminary data shown in Figure 7 by placing the solution in a 5 cm cell and positioned at the focus of a 20 cm radius spherical lens. The light transmitted through the cell was collected by another 20 cm lens and the collimated output directed into a detector. The input power was monitored by directing a portion of the incident power into another detector. The incident wavelength was 532 nm at a pulse width of 10 nsec, and the zero-power transmittance of the solution was 32.2%. At an incident average power of 300 mW the transmittance dropped to 0.9%. The solution exhibited no bleaching and therefore no hysteresis was observed on cycling the incident power.

It is advantageous to extend the range of nonlinear behavior to any portion of the common laser sources. This may be best accomplished by chemically sub-

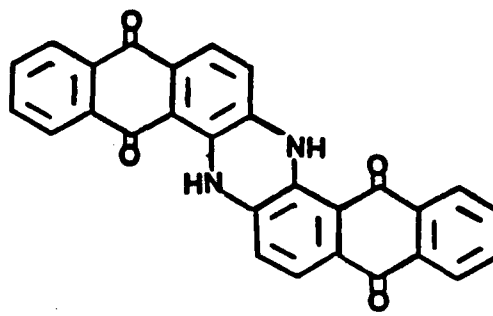
stituting various chromophores on the aromatic portion of the indanthrone molecule (Compound I). The incident intensity required to induce reverse saturable in the parent compound absorption is usually quite high, typically on the order of 10^6 to 10^8 W/cm², and it is desirable to reduce these values as much as possible. One approach we investigated to increase the rate of intersystem crossing between the singlet excited state and the triplet excited state responsible for the excited state absorption. This is usually accomplished by halogenation with -Br or -Cl. This increases the excited state absorption cross section, and effectively reduces the power density required to observe the onset of nonlinear behavior. The spectral range of absorption can be changed by substitution of various chromophores, such as -CH₃ or -NO₂ on the indanthrone molecule, or by extending or rearranging the ring systems of the indanthrone molecule.

Examples of substituted indanthrone systems, rearranged ring systems, and extended ring systems that will be synthesized are shown in Figures 8 through 13. In one example, the synthesis of the 3,3'-dibromo derivative of indanthrone can be accomplished by the condensation of two molecules of 1,3-dibromo-2-aminoanthraquinone, as shown in Figure 8. Also, derivatives containing -Cl, -NO₂, -NH₂, and -Br, in the 5-position were made, as shown in Figure 9 (Compound III).

The linear indanthrone isomers, Compounds IV and V, shown in Figure 10, should exhibit shifts in absorption maxima that may coincide more closely with the emission wavelengths of common laser sources. These linear isomers can undergo substitution and oxidation reactions that may increase their nonlinearity. It is reported that Compound IV can be oxidized with HNO₃ to form the oxidized product (Compound V) shown in Figure 10. This oxidation reaction can also be performed on the parent indanthrone molecule to form the product shown

in Figure 11 (Compound VI). Compound IV can also be brominated to form Compound VII, as described in Figure 12 [21].

Several analogues of indanthrone that we believe exhibit interesting optical properties are shown in Figure 13. Compound VIII is an extended ring system (ladder oligomer) that shift the absorption maxima, and non-linear behavior, into the near infrared region. Potentially, many anthraquinone units may be linked in this fashion forming a highly stable polymeric optical switches. Oligomers of indanthrone and its derivatives (bis-indanthrone amine) were also synthesized (Compound IX), opening the possibility that different indanthrone derivatives with varying optical properties were developed.



Compound I

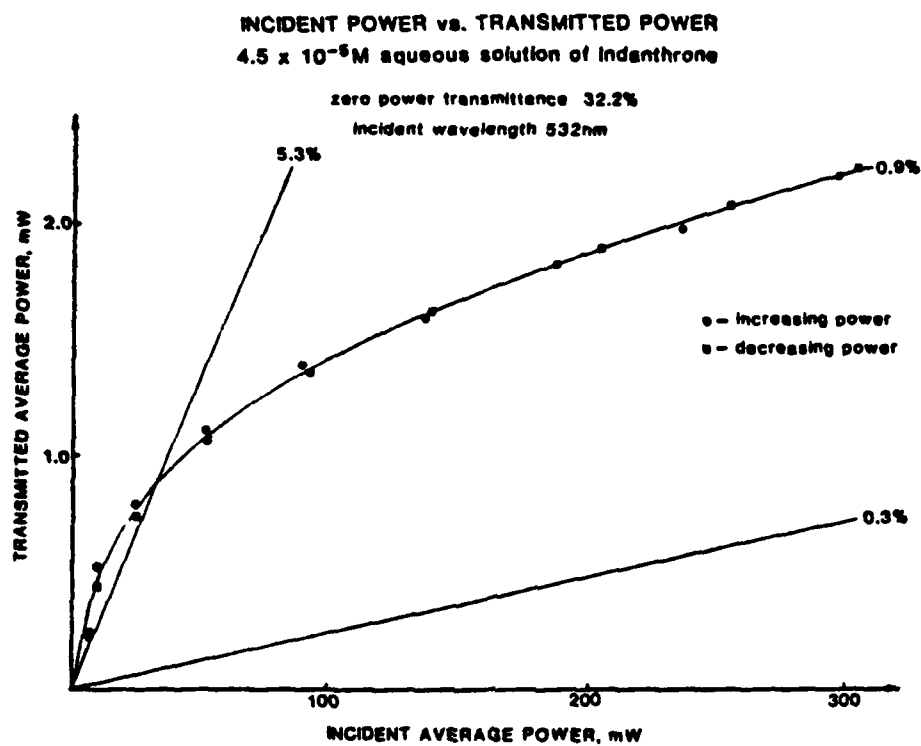


Fig. 3 Nonlinear optical properties of indanthrone.

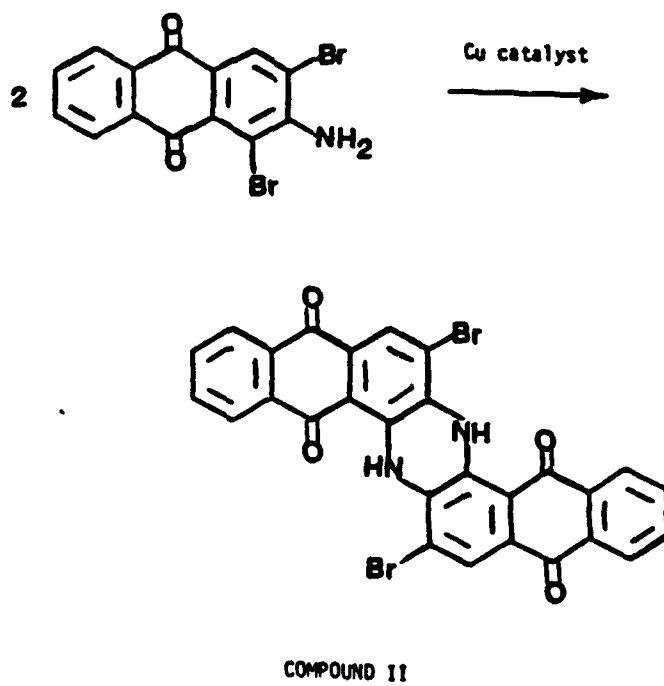
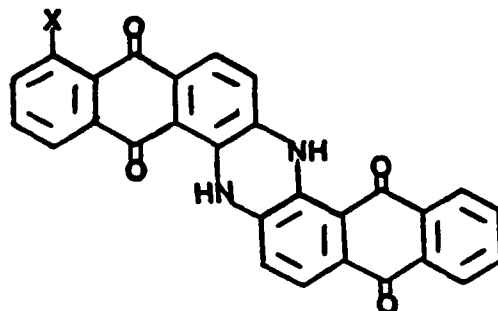


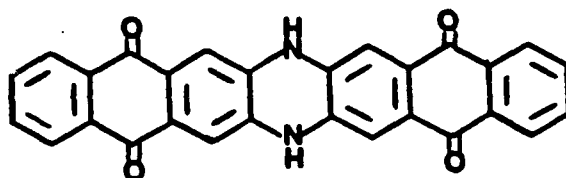
Fig. 4 Synthesis of 3,3'-Dibromoanthraquinone.



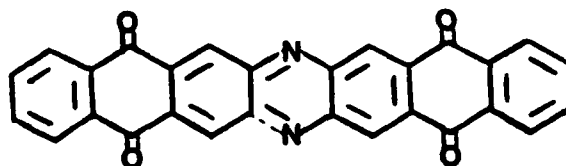
X = -Br, -Cl, -NH₂, -NO₂, -CN

COMPOUND III

Fig. 5 Derivatives of indanthrone substituted on the 5-position

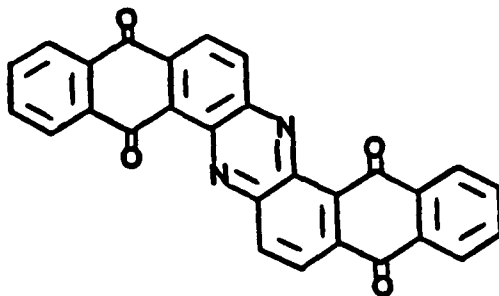


COMPOUND IV



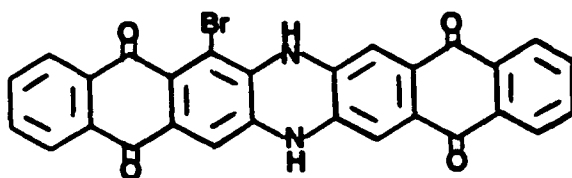
COMPOUND V

Fig. 6 Linear isomers of indanthrone



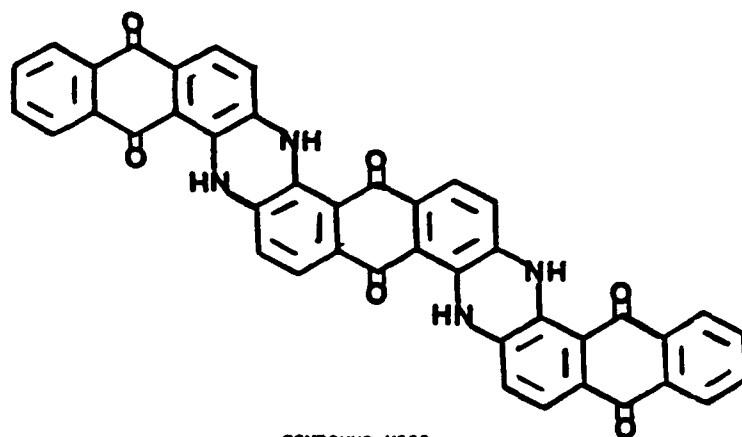
COMPOUND VI

Fig. 7 Oxidized form of indanthrone

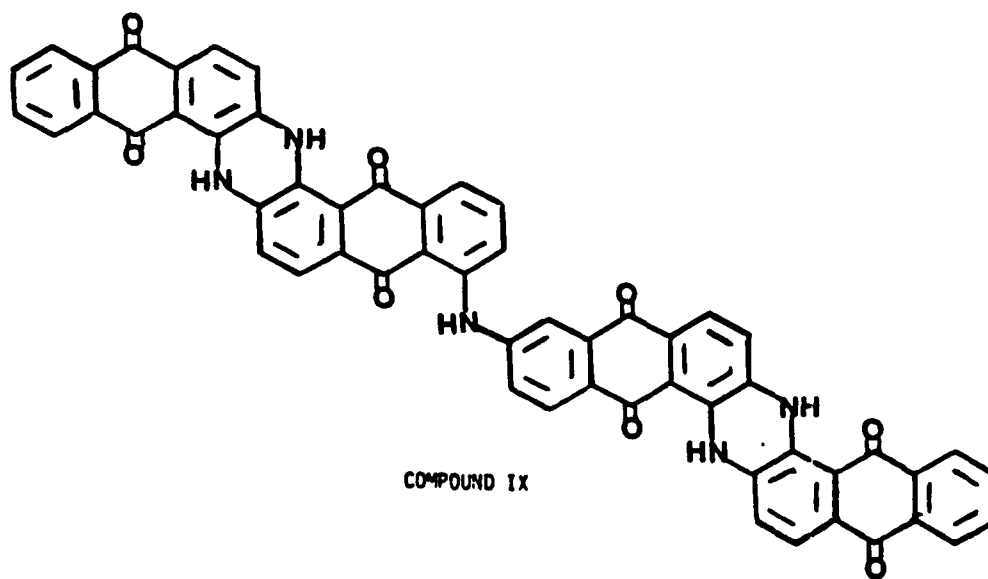


COMPOUND VII

Fig. 8 Bromination of linear form of indanthrone.



COMPOUND VIII



COMPOUND IX

Fig. 9 Indanthrone ladder oligomer and bis-indanthrone amine.

REFERENCES

- [1] Garito, A.F. and Singer, K.D., *Laser Focus* 80 (1982) 59.
- [2] Neff, J.A., *Optical Engineering* 26 (1987) 2.
- [3] Marom, E., *Optical Engineering* 25 (1986) 274.
- [4] Smith, S.D., Walker, A.C., Tooley, F.A.P., Mathew, J.G.H., and Taghizadeh, M.R., Demonstration of a Triple Bistable-Element Loop circuit for a digital Parallel All-Optical Computer, in: Gibbs, H. M., Mandel, P., Peyghambarian, and Smith, S.D., *Optical Bistability III* (Springer-Verlag, 1986) pp. 8-11.
- [5] Bigot, J.Y., Daunois, A., Leonelli, R., Sence, M., Mathew, J.G.H., Smith, S.D., and Walker, A.C., *Appl. Lett.* 49 (1986) 844.
- [6] Hulin, D., Mysyrowicz, A., Antonetti, A., Migus, A., Masselink, W.T., Morkoc, H., Gibbs, H.M. and Peyghambarian, N., *Appl. Phys. Lett.* 49 (1986) 749.
- [7] Szabo, A., U.S. Patent 3,896,420.
- [8] Potember, R.S., Hoffman, R.C., Poehler, T.O., *Johns Hopkins APL Technical Digest* 7 (1986) 129.
- [9] Potember, R.S., Poehler, T.O., and Benson, R.C., *Appl. Phys. Lett.* 41 (1982) 548.
- [10] Benson, R.C., Hoffman, R.C., Potember, R.S., Bourkoff, E., and Poehler, T.O., *Appl. Phys. Lett.* 42 (1983) 855.
- [11] Potember, R.S., Hoffman, R.C., Benson, R.C., and Poehler, T.O., *J. De Physique* 44 (1983) C3-1597.
- [12] Poehler, T.O., Potember, R.S., Hoffman, R.C., and Benson, R.C., *Mol. Cryst. and Liq. Cryst.* 107 (1984) 91.
- [13] Potember, R.S., Poehler, T.O., Hoffman, R.C., Speck, K.R., Benson, R.C., *Molecular Electronics*, Carter, F.L., (ed.), to be published (1986).
- [14] Speck, K.R., Poehler, T.O., and Potember, R.S., *ICALEO Technical Digest* (1986).
- [15] Melby, L.R., Harder, R.J., Hertler, W.R., Mahler, W., Benson, R.E., and Mochel, W.E., *J. Amer. Chem. Soc.* 84 (1962) 3374.
- [16] Kamaras, K., Gruner, G., Sawatzky, G.A., *Solid State Commun.* 27 (1978) 1171.
- [17] Torrance, J.B., Scott, B.A., and Kaufman, E.B., *Solid State Commun.* 17 (1975) 1369.
- [18] Giuliano, C.R., and Hess, L.D., *IEEE Journal of Quantum Electronics*, QE-3 (1967) 358.

- [19] Fieser, L. F. and Fieser, M., Topics on Organic Chemistry, Reinhold Publishers (New York, 1963) p. 381.
- [20] Giuliano, C. R. and Hess, L. D., IEEE J. Quantum Elec. (1966), 338-367.
- [21] Clark, M. C., J. Chem. Soc. (C) (1966), 2090-2095.

V. SYNTHESIS OF NOVEL MATERIALS FOR LARGE SCALE ELECTRICAL AND OPTICAL NETWORKS

A. Summary of Progress

A search is currently underway for organic complexes with the most promising potential for use in a large-scale electrical or optical networks. It has been shown that radical ion acceptors such as the TCNQ compounds with different substituents on the parent structure undergo electron transfer at different applied energies [1-6]. Synthetic chemical work is underway to produce a variety of the most interesting and useful of these compounds. Ample supplies of the compounds discussed below are now available for use in physical, electronic, and structural testing.

Significant progress has been made on the organic synthesis in the development of new and advanced materials to support this program. During the past three years, efforts have concentrated on designing and synthesizing novel organic compounds and polymers for electronic and optical devices.

The chemistry of TCNQ provides many options because it is possible to custom tailor the acceptor molecule to suit specific electronic and/or optical requirements. For example, TCNQ·F₄ has a high switching threshold and it could possibly be used as an electrical switch, while TCNQ·(OCH₃)₂ has a low threshold, and may be more suitable for an erasable optical processing system.

Synthetic chemical work in the past has produced a variety of interesting new compounds. TNAP and TCNQ·F₄ have been made using known or novel synthetic routes. Ample supplies of these compounds are currently available for use in physical, electronic, and optical evaluation. Other compounds such as TCNQ·(OCH₃)₂, TCNQ·Br₂ and TCNQ·(O-Phenyl)₂ have been produced.

Work in the laboratory to support the overall goal of this research program by providing new materials for use in the investigation of TCNQ-based systems

has been completed. Below, areas of investigation that were under extensive study are summarized.

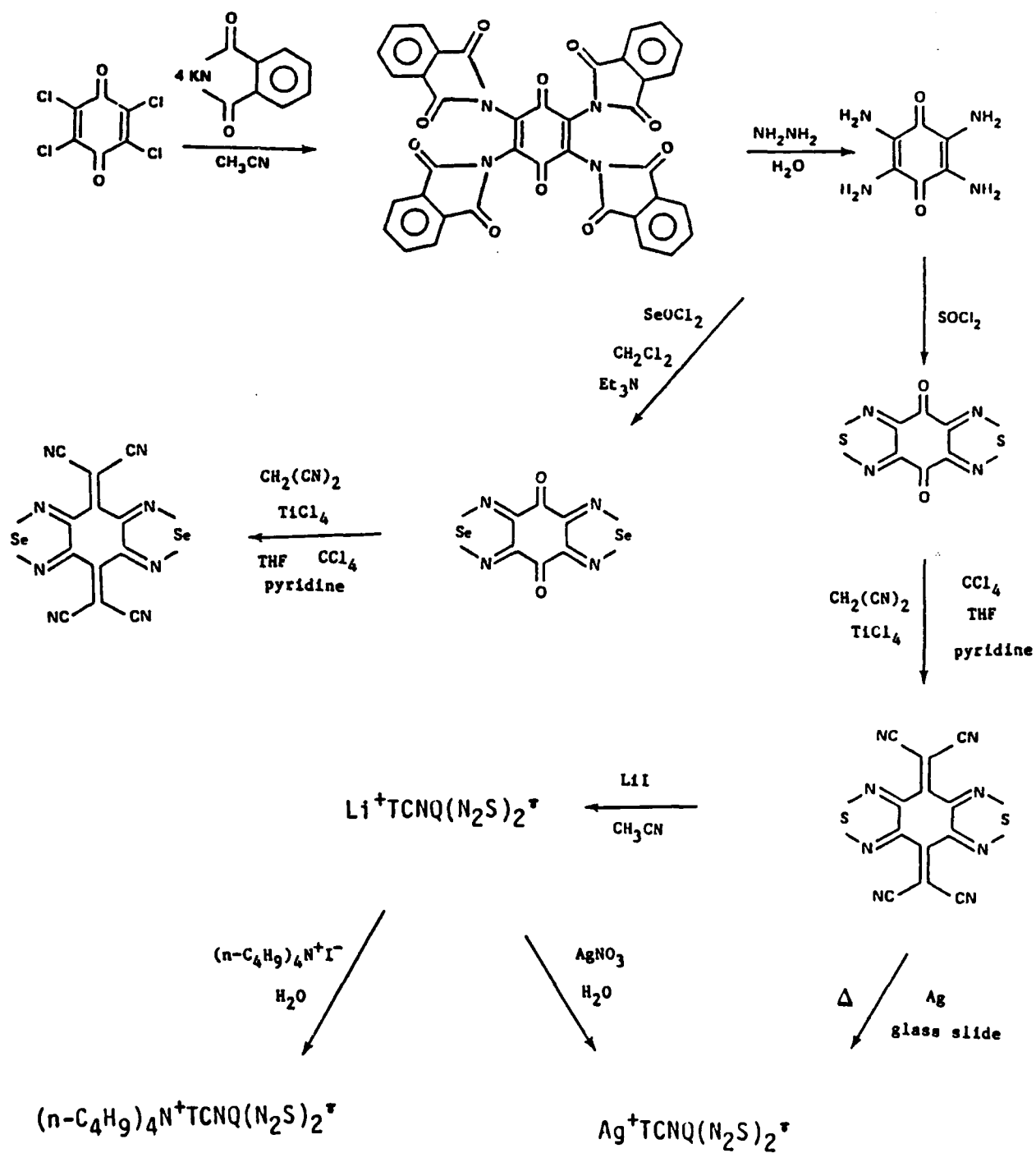
(A) Study of Bis[1,2,5]thiadiazolo-tetracyanoquinodimethane, BTDA-TCNQ or TCNQ(N₂S)₂.

We have prepared and characterized the compound TCNQ(N₂S)₂, the novel organic acceptor that contains dye-like chromophores chemically bonded to the parent benzenoid TCNQ structure first reported briefly as a communication in 1985 [7] and in our last report.

It has been shown that TCNQ(N₂S)₂ has several advantages in forming highly conductive complexes with donors such as tetrathianaphthalene. Unlike 11,11,12,12-tetracyanoanthraquinodimethane (TCNAQ) and [1,2,5]thiadiazolo-tetracyanonaphthoquinodimethane (TDA-TCNNQ) which are non-planar due to the steric interaction between the dicyanomethylene groups and peri-hydrogen atoms, TCNQ(N₂S)₂ is planar and symmetrical. Furthermore, the thiadiazole rings can stabilize the anion radical by conjugation as well as by the resonance contribution generating a new aromatic sextet, and heteroatoms in the thiadiazole rings may increase the interaction between the outside and the inside of the stack in the complex.

The preparation of TCNQ(N₂S)₂ is shown in Scheme I. The compound is prepared by the following general procedure:

A mixture of tetrachloro-1,4-benzoquinone and potassium phthalimide in dry acetonitrile was refluxed to yield tetraphthalimido-1,4-benzoquinone (84%), which was then treated with 80% hydrazine to give a black powder crystal of tetraamino-1,4-benzoquinone (80%). Condensation of tetraamino-1,4-benzoquinone with freshly distilled thionyl chloride at 82 °C gave a light brown shiny flake of 4H,8H-benzo[1,2-c:4,5-c']-bis[1,2,5]thiadiazolo-4,8-dione (47%) which was then condensed with malononitrile using titanium tetrachloride as a catalyst to give TCNQ(N₂S)₂ in 61% yield. Refluxing of TCNQ(N₂S)₂ with anhydrous lithium iodide in dry acetonitrile gave Li⁺TCNQ(N₂S)₂⁻ (57%), which was then used to exchange with silver nitrate and tetra-n-butylammonium iodide, respectively, in water to give salts of Ag⁺TCNQ(N₂S)₂⁻ (78%) and (n-C₄H₉)₄N⁺TCNQ(N₂S)₂⁻ (74%).



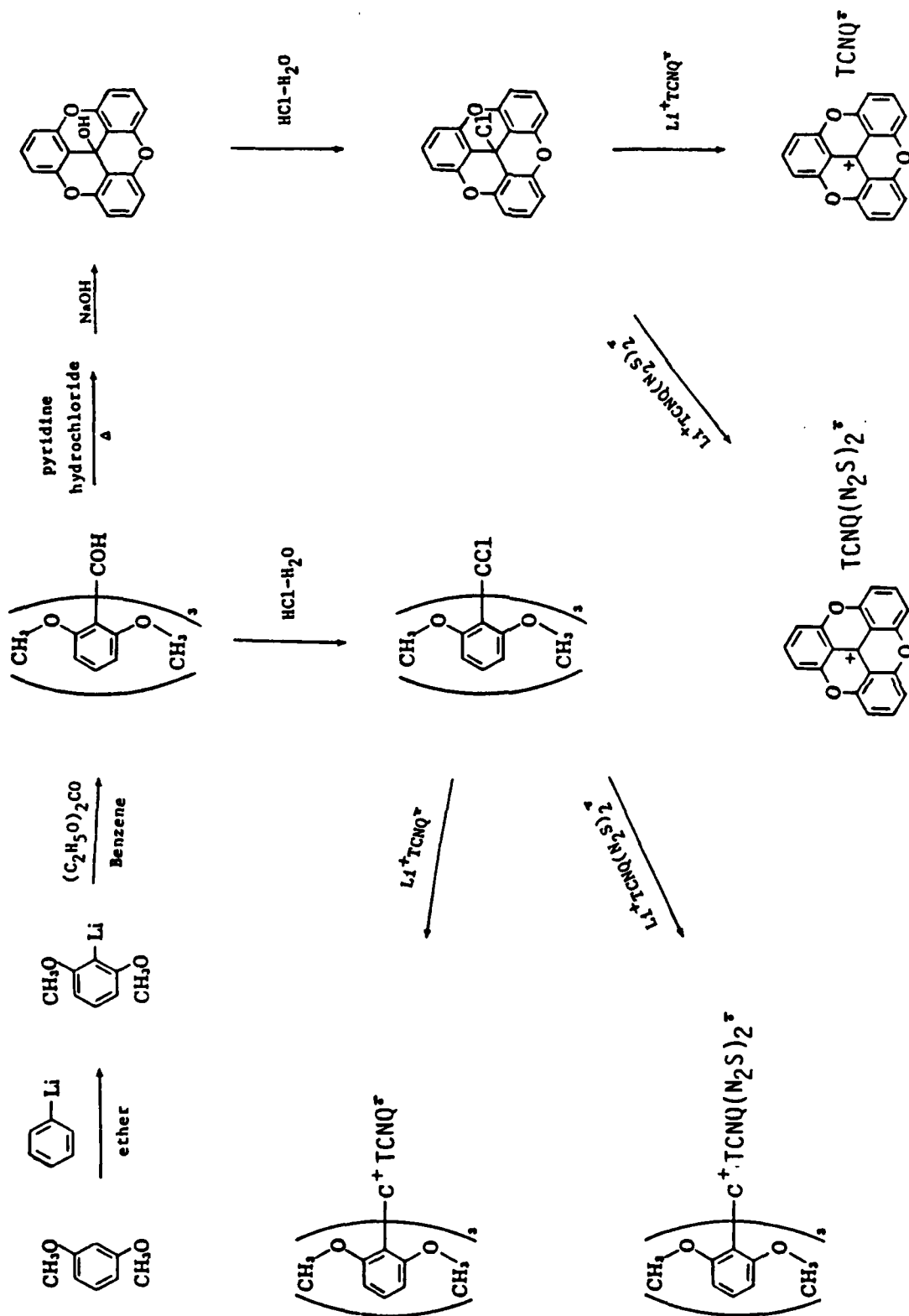
Scheme I

We have worked to prepare the selenium and tellurium analogs, namely, $\text{TCNQ}(\text{N}_2\text{Se})_2$ and $\text{TCNQ}(\text{N}_2\text{Te})_2$, by replacing SOCl_2 with SeOCl_2 and TeOCl_2 , respectively (see Scheme I). Initial experiments involving condensation of tetraamino-1,4-benzoquinone in dry methylene chloride and triethylamine with selenium oxydichloride gave a fine mustard yellow powder in 11% yield, which was then reacted with malononitrile by a TiCl_4 -catalyzed condensation to give a mustard yellow powder (62%). The characterization of $\text{TCNQ}(\text{N}_2\text{Se})_2$ is in progress. Literature reports of this compound have not been complete. We are working to obtain an acceptable charalysis.

In addition to the successful wet preparation of $\text{Ag}^+\text{TCNQ}(\text{N}_2\text{S})_2^-$, we have attempted to prepare the charge-transfer complex $\text{Ag}^+\text{TCNQ}(\text{N}_2\text{S})_2^-$ as a thin film on a glass slide using a sublimation/solid state reaction technique developed in this laboratory. A glass slide with a thin layer of neutral $\text{TCNQ}(\text{N}_2\text{S})_2$ on silver was heated at 275°C for a period of 10 sec resulting in a bluish green thin film. The chemical change has been characterized by reflectance infrared spectra, which indicates that decomposition took place at 275°C before or after the formation of a charge-transfer complex $\text{Ag}^+\text{TCNQ}(\text{N}_2\text{S})_2^-$. Further studies need to be continued.

In an effort to grow high quality large crystals of these TCNQ-based derivatives for X-ray structural analysis and conductivity measurements, electrocrystallization of $\text{TCNQ}(\text{N}_2\text{S})_2$ and CuBr_2 in dry acetonitrile in a cell furnished with two Pt electrodes and constant current density has been employed. A modified cyclic voltametric measurement apparatus was set up to determine the voltage at which the cation will oxidize.

To compare $\text{TCNQ}(\text{N}_2\text{S})_2$ with the parent TCNQ for potential use in optical switching studies, UV/visible absorbance spectra in acetonitrile solutions were obtained. Neutral TCNQ has a single peak at 384 nm while neutral $\text{TCNQ}(\text{N}_2\text{S})_2$ has



Scheme II

peaks at 382, 362, 306, and 237 nm. In contrast, $\text{Li}^+\text{TCNQ}^\ominus$ has new peaks at 840, 822, 758, 741 and 678 nm while $\text{Li}^+\text{TCNQ}(\text{N}_2\text{S})_2^\ominus$ has new peaks at 623, 571, and 525 nm. From these results, $\text{TCNQ}(\text{N}_2\text{S})_2$ appears to have a lower threshold due to the fusion of the TCNQ moiety with 1,2,5-thiadiazole unit. Apparently the thia-diazole unit stabilizes the anion radical by conjugation as well as by the resonance contribution generating a new aromatic sextet.

(B) Study of Sesquixanthrol and its application for reversible photostimulated dilation.

We have prepared and characterized sesquixanthrol [8]. Because its derivative carbonium ion, being capable of attaining complete coplanarity and complete planar symmetry, may have the advantage of forming a highly conductive complex with acceptors (see Scheme II). Furthermore, the charge delocalization on the whole system by conjugation on the carbonium ion and the large molecular size may increase the interaction between the outside and the inside of the stack in the complex, hence increasing the electrical conductivity. In addition, this kind of organic donor is soluble in many solvents in both its reduced and oxidized form, while a metallic donor is insoluble in any solvent in its reduced form when optical switching of its charge-transfer complex occurs.

By the method outlined in Scheme II, this organic donor molecule was prepared according to the procedure of Martin and Smith, and from which the new CT-complexes were generated.

Phenyllithium was freshly prepared from the addition of bromobenzene in ether to lithium wire in ether, and 1,3-dimethoxybenzene was added to give 1,3-dimethoxymethyl-lithium-2 due to translithiation. Furthermore, the addition of diethyl carbonate in benzene and subsequent treatment with water gave 2,6,2',6',2'',6''-hexamethoxytriphenylcarbinol (39%). Cyclization took place when the mixture of pyridine hydrochloride and 2,6,2',6',2'',6''-hexamethoxytriphenylcarbinol was heated at 205 °C to give the title compound, sesquixanthrol (28%).

The suspension of 2,6,2',6',2'',6'''-hexamethoxytriphenylcarbinol in water was reacted with 10% hydrochloric acid to generate a clear purple solution, which was then treated with aqueous solution of $\text{Li}^+\text{TCNQ}^\ominus$ and $\text{Li}^+\text{TCNQ}(\text{N}_2\text{S})_2^\ominus$, respectively, to give the CT-complexes of 2,6,2',6',2'',6'''-hexamethoxytriphenylcarbonium $^+\text{TCNQ}^\ominus$ (97%) and 2,6,2',6',2'',6'''-hexamethoxytriphenylcarbonium $^+\text{TCNQ}(\text{N}_2\text{S})_2^\ominus$ (97%). Following the same procedure, sesquixanthydryl $^+\text{TCNQ}^\ominus$ (84%) and sesquixanthydryl $^+\text{TCNQ}(\text{N}_2\text{S})_2^\ominus$ (92%) were prepared from sesquixanthydrol.

Verification of the products was performed using IR transmittance and UV/visible absorbance spectra of the respective anion radicals.

Sesquixanthydryl $^+\text{TCNQ}^\ominus$ and 2,6,2',6',2'',6'''-hexamethoxytriphenylcarbonium $^+\text{TCNQ}^\ominus$ have peaks similar to $\text{Li}^+\text{TCNQ}^\ominus$, while sesquixanthydryl $^+\text{TCNQ}(\text{N}_2\text{S})_2^\ominus$ and 2,6,2',6',2'',6'''-hexamethoxytriphenylcarbonium $^+\text{TCNQ}(\text{N}_2\text{S})_2^\ominus$ have peaks similar to $(n\text{-C}_4\text{H}_9)_4\text{N}^+\text{TCNQ}(\text{N}_2\text{S})_2^\ominus$. Stability of this new organic donor in the reduced form requires further study.

It has been shown that the sesquixanthydryl radical provides a minimum of steric hindrance to dimerization, and the postulated coplanar structure of the radical provides the optimum geometry for delocalization of the odd electron, while the 2,6,2',6',2'',6'''-hexamethoxytriphenylmethyl radical, bearing six orthomethoxy substituents, is expected to have a relatively large angle of twist of the phenyl groups in its most stable conformation, which would reduce the resonance stabilization of the radical, hence a large steric hindrance to dimerization due to extreme steric crowding is expected.

References

1. R. S. Potember, R. C. Hoffman, R. C. Benson, and T. O. Poehler, "Erasable Optical Switching in Semiconductor Organic Charge-transfer Complexes," *J. Phys. (Paris)*, Vol. 44, pp. C3-1597-1604 (1983).
2. R. S. Potember, T. O. Poehler, R. C. Hoffman, K. R. Speck, and R. C. Benson, "Reversible Electric Field Induced Bistability in Carbon Based Radical-Ion Semiconducting Complexes: A Model System for Molecular Information Processing and Storage," 2nd International Workshop on Molecular Electronic Devices, edited by F. L. Carter, (Marcel Dekker, Inc., NY) 1985.
3. R. S. Potember, T. O. Poehler, K. R. Speck, R. C. Hoffman, and C. A. Viands, "Bistable Optical Threshold Switching in Organic Photochromic Materials," *Bull. Am. Phys. Soc.*, Vol. 31, p. 657 (1986).
4. R. C. Hoffman, T. O. Poehler, and R. S. Potember, "Characterization of an Erasable Organometallic Optical Storage Medium," Conf. on Lasers and Electro-optics - Technical Digest, p. 358 (1986).
5. R. S. Potember, R. C. Hoffman, and T. O. Poehler, "Molecular Electronics," *Johns Hopkins APL Tech. Digest*, Vol. 7, No. 2, p. 129 (1986).
6. R. S. Potember, R. C. Hoffman, H. Hu, J. E. Cocchiaro, C. A. Viands, and T. O. Poehler, "Electronic Devices from Conducting Organics and Polymers," *Polymer J. (Japan)*, Vol. 19, pp. 147-156 (1987).
7. Y. Yamashita, T. Suzuki, T. Mukai, and G. Saito, "Preparation and Properties of a Tetracyanoquinodimethane Fused with 1,2,5-Thiadiazole Units," *J. Chem. Soc., Chem. Commun.*, pp. 1044-1045 (1985).
8. J. C. Martin and R. G. Smith, "Factors Influencing the Basicities of Triarylcarbinols. The Synthesis of Sesquixanthrol," *J. Am. Chem. Soc.*, Vol. 86, pp. 2252-2256 (1964).

B. Experimental Section

Tetraphthalimido-1,4-benzoquinone: Tetrachloro-1,4-benzoquinone (100 g, 0.41 mole) and potassium phthalimide (312 g, 1.68 mole) were mixed with 2 L of dry acetonitrile (distilled over phosphorus pentoxide two times and calcium hydride one time) in a 3 L three-necked round-bottomed flask equipped with a mechanical stirrer and a reflux condenser under nitrogen. The resulting mixture was heated to reflux overnight, cooled to room temperature and placed in an ice-water bath for 3 hours. After filtering through a sintered-glass funnel, the solid mass was washed with 90 °C water 3 x 1000 mL, dried, ground into powder and transferred into a 3 L three-necked round-bottomed flask equipped with a mechanical stirrer. With the addition of ethanol 1 L, the mixture was heated to boil for 10 min and hot filtered. The solid was dried on a rotatory evaporator at 65 °C under the water aspirator pressure, ground into powder and further dried in vacuo at 80 °C for 3 hours to give a tan colored powder 234.2 g, yield 84%, mp > 400 °C. IR(KBr) 1787, 1733, 1683, 1621, 1557, 1467, 1375, 1360, 1243, 1177, 1082, 965, 877, 793, 777, 743, 713, 667 cm^{-1} .

Tetraamino-1,4-benzoquinone: In a 3 L three-necked round-bottomed flask equipped with a mechanical stirrer, a reflux condenser and a pressure-equalized dropping funnel were placed tetraphthalimido-1,4-benzoquinone (186 g, 0.27 mole) and 900 mL of water. While the flask was cooled in an ice-water bath, hydrazine (1 L, 80%) was added dropwise over a period of 2 hours through the dropping funnel. Mechanical stirring was continuing at room temperature for 1 hour, at 50 °C for 3 hours, and at room temperature overnight. The flask was cooled in an ice-water bath for 3 hours and the solid was collected on a filter and washed thoroughly with water 2 x 400 mL and ethanol 3 x 50 mL. The solid was ground finely, dried on a rotatory evaporator at 85 °C under the water aspirator pressure for 2 hours, and further dried in vacuo at 85 °C for 2 hours to give a

bright metallic black powder crystal 36.2 g, yield 80%, mp not observed (decomposition started at 200 °C). IR(KBr) 3450-3050 (-NH₂), 1645 (C=O), 1522 (C=C), 1375, 1133, 832, 724, 660, 550 cm⁻¹.

4H,8H-benzo[1,2-c:4,5-c']bis[1,2,5]thiadiazole-4,8-dione: Tetraamino-1,4-benzoquinone (6.72 g, 0.04 mole) and 75 mL of dry freshly distilled thionyl chloride were refluxed for 24 hours in an oil bath at 82 °C as the top of the condenser was provided with a drying tube packed with Drierite. The unreacted thionyl chloride was distilled off slowly at 40-55 °C under the water aspirator pressure with the protection of a drying tube. The residue was concentrated to dryness in vacuo at 60 °C, ground into powder and further dried to a constant weight. The crude product was purified by hot filtration with 5 g of freshly activated carbon (heated at 130 °C overnight) and N,N'-dimethylformamide 2 x 100 mL. The filtrate was placed at 0 °C overnight. The product was collected on a filter, washed with 10 mL of N,N'-dimethylformamide and dried in vacuo to give a light brown shiny flake 4.23 g, yield 47%, mp > 400 °C (crystal built up on the top glass wall). UV/visible (CH₃OH): λ_{max} (lg ε) = 221 (3.76), 263 (3.67), 294 nm (3.94). IR(KBr) 1705 (C=O), 1450 (C=N), 1405, 1333, 1321, 1058, 1046, 860, 843, 748, 673, 510 cm⁻¹.

Bis[1,2,5]thiadiazolo-tetracyanoquinodimethane, BTDA-TCNQ or TCNQ(N₂S)₂: A solution of titanium tetrachloride (1.69 g, 8.9 mmole) in 3 mL of dry carbon tetrachloride (distilled over phosphorus pentoxide) was added dropwise to 20 mL of dry tetrahydrofuran (predried over sodium hydroxide, then distilled through benzophenone ketyl) in a 100 mL three-necked round-bottomed flask in an ice-water bath under nitrogen to give a yellow flaky precipitate in 5 min. While the temperature was maintained at 0 °C, a solution of malononitrile (0.40 g, 6.1 mmole) in 5 mL of dry tetrahydrofuran was added over a period of 1 min, 4H,8H-benzo[1,2-c:4,5-c']bis[1,2,5]thiadiazole-4,8-dione (0.50 g, 2.2 mmole) was added at one time, and a solution of 1.4 mL of dry pyridine (distilled over

sodium hydroxide) in 3 mL of dry tetrahydrofuran was added dropwise in 3 min. Stirring was continuing at 0 °C for 1 hour and at room temperature overnight to give a gray yellow precipitate. While the flask was maintained in an ice-water bath, 50 mL of water was added dropwise in 10 min and stirred for an additional 20 min. The solid was collected on a filter, washed with pentane, and dried in vacuo at 100 °C to give a gray yellow powder 0.45 g, yield 63%, mp 367-372 °C (dec.) (lit. 375-380 °C, dec.). UV/visible (CH₃CN): λ_{\max} (lg ϵ) = 236.9 (4.03), 306.7 (4.38), 362.0 (4.46), and 381.8 nm (4.50). MS(70 eV): m/e(%) = 322(M⁺,29), 321(100), 320(62), 296(2), 295(3), 269(2), 257(2), 219(3), 218(3), 193(14), 192(3), 161(7), 160(7), 146(4), 128(3), 116(12), 64(60), 32(97). IR(KBr) 2235 (C≡N), 1578 (C=C), 1461 (C=N), 1427, 1307, 1207, 1118, 1028, 849, 834, 584 cm⁻¹. TCNQ: IR (thin Film) 2224 (C≡N), 1549 (C=C), 1406, 1354, 1208, 1127, 999, 963, 860 cm⁻¹. UV/visible (CH₃CN): λ_{\max} (lg ϵ) = 384.

Li⁺TCNQ(N₂S)₂⁻: In a 25 mL of three-necked round-bottomed flask equipped with a reflux condenser under nitrogen was placed a boiling clear solution of TCNQ(N₂S)₂ (50 mg, 0.156 mmole) in 10 mL of dry acetonitrile. A clear solution (boiled for 5 min and cooled to room temperature) of anhydrous lithium iodide (63 mg, 0.468 mmole) in 5 mL of dry acetonitrile was added dropwise over a period of 3 min. The color of the resulting mixture changed rapidly to a deep green. The flask was heated to reflux for 2 hours and placed at room temperature for 1 hour. The product was collected on a filter, washed with dry acetonitrile and dried in vacuo at 100 °C to give a black solid, 40 mg, yield 78%, mp > 400 °C. UV/visible (CH₃CN): λ_{\max} (lg ϵ) = 622.7 (4.38), 570.6 (4.04), 524.8 (3.57), 371.4 (4.03), 343.6 (4.12), 300.7 (4.32), and 227.1 nm (3.96). IR(KBr) 2197 (C≡N), 1468, 1439, 1421, 1257, 850 cm⁻¹.

Li⁺TCNQ⁻: IR(KBr) 2196, 1570, 1505, 1323, 1180, 992, 826 cm⁻¹. UV/visible (CH₃CN): λ_{\max} (lg ϵ) = 394, 405, 418, 678, 714, 759, 822, 840.

(n-C₄H₉)₄N⁺TCNQ(N₂S)₂⁻: To a clear solution of Li⁺TCNQ(N₂S)₂⁻ (15 mg, 0.034 mmole) in 1 mL of water stirring at room temperature, a hot solution (boiled for 2 min) of tetra-n-butylammonium iodide (12.4 mg, 0.034 mmole) in 1 mL of water was added by portions over a period of 1 min to give a precipitate. The flask was heated to reflux for 20 min and allowed to stand at room temperature overnight. The solid was collected on a filter, washed with water and dried in vacuo at 100 °C to give a dark blue powder 17 mg, yield 74%, mp 138-140 °C (dec.). UV/visible (CH₃CN): λ_{max} (lg ε) = 225 (4.14), 300 (4.45), 335 (4.37), 370 (4.20), 525 (4.00), 570 (4.16), 628 nm (4.49). IR(KBr) 2181 (C≡N), 1458, 1395, 1348, 1278, 1168, 886, 838, 731, 671, 610 cm⁻¹.

(n-C₄H₉)₄N⁺TCNQ⁻: To a clear solution of Li⁺TCNQ⁻ (845 mg, 4 mmole) in 10 mL of water stirring at room temperature, a hot solution (boiled for 2 min) of tetra-n-butylammonium iodide (1480 mg, 4 mmole) in 25 mL of water was added dropwise in 10 min to give a precipitate. The flask was heated to reflux for 20 min and allowed to stand at room temperature overnight. The solid was collected on a filter, washed with water and dried in vacuo at 100 °C to give a dark blue powder 1.7 g, yield 95%, mp 113-117 °C (dec). IR(KBr) 2903, 2875, 2184 (C≡N), 1583, 1508, 1468, 1363, 1183, 993, 831 cm⁻¹. UV/visible (CH₃CN): λ_{max} (lg ε) = 233 (3.87), 261 (3.57), 409 (4.22), 420 (4.25), 665 (3.67), 680 (3.75), 743 (4.20), 761 (4.14), 824 (4.32), 843 nm (4.46).

Attempted Preparation of Ag⁺TCNQ(N₂S)₂⁻ on a Glass Slide: Silver was heated to sublime and allowed to deposit a thin film on a glass slide 1" x 1" at 10⁻⁶-10⁻⁷ mm Hg. TCNQ(N₂S)₂ powder was heated to sublime at 10⁻⁶-10⁻⁷ mm Hg and allowed to deposit a yellow thin film on the silver glass slide. The slide was placed on a hot plate at 275 °C for a period of 10 sec resulting in a bluish green thin film. Reflectory IR: (before heating) 3067, 3051, 2228, 1580, 1543, 1462, 1429, 864, 847, 831 cm⁻¹; (after heating) 2234, 1582, 1462, 1427, 867, 831 cm⁻¹.

Ag⁺TCNQ(N₂S)₂⁻: To a clear dark blue solution of Li⁺TCNQ(N₂S)₂⁻ (55 mg, 0.168 mmole) in 1.5 mL of water stirring at room temperature, a colorless solution of silver nitrate (30 mg, 0.176 mmole) in 1.5 mL of water was added by portions which yielded instantly a precipitate. The mixture was stirred at room temperature for 1 h and allowed to stand in an ice-water bath for 2 h. The solid was collected on a filter, washed with water and dried in vacuo at 100 °C to give a gray powder 56 mg, yield 78%, mp 330-340 °C (dec.), (crystal built up on the top glass wall). IR(KBr) 2180 (C≡N), 1460, 1430, 1408, 1260, 845, 832 cm⁻¹. UV/visible (CH₃CN): λ_{max} (lg ε) 227 (4.19), 245 (4.12), 261 (4.10), 299 (4.49), 306 (4.48), 363 (4.41), 382 (4.45), 527 (3.10), 574 (3.35), 631 nm (3.69).

4H,8H-benzo[1,2-c:4,5-c']bis[1,2,5]selenadiazole-4,8-dione: In a 500 mL three-necked round-bottomed flask equipped with a reflux condenser and a pressure-equalized dropping funnel under nitrogen was placed a suspension of tetraamino-1,4-benzoquinone (1.90 g, 11.3 mmole) in 300 mL of dry methylene chloride (predried over activated alumina and distilled over calcium hydride) and 24 mL of dry triethylamine (predried over 4A molecular sieves and distilled over lithium aluminum hydride) in an ice-water bath. A solution of selenium oxydichloride (5.60 g, 33.7 mmole) in 20 mL of dry methylene chloride was added dropwise over a period of 1 hour. The resulting mixture was stirred at room temperature for 1 hour, heated to reflux for 4 hours and stirred at room temperature overnight. The crude product collected on a filter was a mixture of a dark brown solid and a shiny bright crystal. The crystal impurity was washed out with 125 mL of methylene chloride. The resulting dark brown mass was further purified by hot filtration with 2 g of activated carbon and N,N'-dimethylformamide 2 x 80 mL. The filtrate was placed at 0 °C overnight. The crude product was collected on a filter, washed with methylene chloride to give a yel-

low crystal mixed with a yellow powder. The mixture was further dried in vacuo at 100 °C for 30 min to give a fine mustard yellow powder 0.39 g, yield 11%, mp > 400 °C (crystal built up on the top glass wall). IR(KBr) 1710, 1486, 1380, 1065, 755, 435 cm^{-1} . UV/visible (CH_3CN): λ_{max} ($1\text{g } \epsilon$) = 206 (4.35), 232 (3.77), 301 nm (3.77).

Bis[1,2,5]selenadiazolo-tetracyanoquinodimethane BSDA-TCNQ or TCNQ(N₂Se)₂: To a solution of titanium tetrachloride (240 mg, 1.26 mmole) in 1 mL of dry carbon tetrachloride in an ice-water bath under nitrogen, 5 mL of dry tetrahydrofuran was added dropwise to give a yellow flaky precipitate. While the temperature was maintained at 0 °C, a solution of malonitrile (70 mg, 1.06 mmole) in 1 mL of dry tetrahydrofuran was added by portions in 1 min, 4H,8H-benzo[1,2-c:4,5-c']-bis[1,2,5]selenadiazole-4,8-dione (100 mg, 0.314 mmole) was added at one time, and a solution of 0.3 mL of dry pyridine in 1 mL of dry tetrahydrofuran was added dropwise over a period of 1 min to give a yellow precipitate in 1 min. Stirring was continuing at room temperature overnight. While the mixture was maintained in an ice-water bath, 10 mL of water was added dropwise over a period of 10 min and the mixture was stirred for an additional 20 min. The solid was collected on a filter, washed with pentane and dried in vacuo at 100 °C to give a mustard yellow powder 81 mg, yield 62%, mp > 400 °C (turned dark brown). IR(KBr) 2239, 1575, 1474, 1410, 1302, 1022, 874, 772, 722 cm^{-1} . UV/visible (CH_3CN): λ_{max} ($1\text{g } \epsilon$) = 242 (4.02), 351 nm (4.55).

2,6,2',6',2'',6''-Hexamethoxytriphenylcarbinol: A solution of phenyllithium was prepared by the dropwise addition of bromobenzene (157.0 g, 1.000 mole) in 500 mL of dry ether over 4 h at room temperature to lithium wire (16.0 g, 2.308 mole) in 240 mL of dry ether in a 2000 mL three-necked round-bottomed flask equipped with a reflux condenser and a pressure-equalized dropping funnel under nitrogen and the mixture was stirred for an additional 6 h. 1,3-Dimethoxy-

benzene (120.0 g, 0.872 mole) was added dropwise in 30 min and the mixture was stirred for an additional 2 h and allowed to stand at room temperature for 3 days. Diethyl carbonate (32.0 g, 0.270 mole) in 1500 mL of dry benzene was added and the reaction mixture was refluxed for 3 days. 1000 mL of water was added and the organic layer was separated, washed with water, dried (Na_2SO_4), decanted and concentrated to give a gray solid. Recrystallization from ether gave a white (lightly tan) needle crystal 52.9 g, yield 39%, mp 160.5-162.5 °C (lit. 163.0-164.5 °C). UV/visible (0.1N HCl): λ_{max} (lg ϵ) = 205 (4.80), 288 (4.52), 356 (4.41), 454 nm (3.98). IR(KBr) 3510(-OH), 3000, 2987, 2835 (C-H), 1587, 1464, 1429, 1395, 1280, 1250, 1167, 1106, 1081, 1031, 1010, 921, 891, 871, 792, 782, 753, 735 cm^{-1} .

2,6,2',6',2'',6'''-Hexamethoxytriphenylcarbonium⁺TCNQ⁻: To a suspension of 2,6,2',6',2'',6'''-hexamethoxytriphenylcarbinol (500 mg, 1.06 mmole) in 10 mL of water stirring in an ice-water bath, 2 mL of 10% aqueous hydrochloric acid (5.4 mmole) was added dropwise which yielded instantly a clear purple solution, to which a clear dark blue solution of Li^+TCNQ^- (224 mg, 1.06 mmole) in 5 mL of water was added dropwise over 2 min to give a precipitate. The mixture was stirred at room temperature overnight and allowed to stand at 0 °C for 2 h. The solid was collected on a filter, washed with 5 mL of water, and dried at 100 °C to give a deep purple powder 678 mg, yield 97%, mp 169-173 °C (dec.). UV/visible (CH_3CN): λ_{max} (lg ϵ) = 209 (4.80), 268 (4.18), 279 (3.99), 339 (3.83), 372 (3.75), 395 (3.90), 480 (4.33), 679, 744, 762, 843 nm. IR(KBr) 3002, 2940, 2845 (C-H), 2185, 2158 (C \equiv N), 1590, 1565, 1559, 1478, 1425, 1362, 1257, 1230, 1105, 805, 749, 631 cm^{-1} .

2,6,2',6',2'',6'''-Hexamethoxytriphenylcarbonium⁺TCNQ(N₂S)₂⁻: To a suspension of 2,6,2',6',2'',6'''-hexamethoxytriphenylcarbinol (79 mg, 0.167 mmole) in 3 mL of water stirring in an ice-water bath, 0.5 mL of 10% aqueous hydrochloric acid

(1.4 mmole) was added dropwise which yielded a clear purple solution, to which a brown solution of $\text{Li}^+\text{TCNQ}(\text{N}_2\text{S})_2^-$ (75 mg, 0.167 mmole) in 5 mL of water was added by portions to give a precipitate. The mixture was stirred at room temperature overnight and allowed to stand for 1 day. The solid was collected on a filter, washed with 3 mL of water, and dried at 100 °C to give a purple powder 140 mg, yield 97%, mp 199-202 °C (dec.). UV/visible (CH_3CN): λ_{max} ($\lg \epsilon$) = 207 (4.85), 267 (4.29), 299 (4.40), 339 (4.18), 358 (4.17), 380 (4.15), 527 (3.52), 574 (3.91), 631 nm (4.18). IR(KBr) 3002, 2940, 2820 (C-H), 2180 (C≡N), 1583, 1463, 1411, 1253, 1093, 1022, 840, 783, 741, 670, 600 cm^{-1} .

Sesquixanthrol: Pyridine hydrochloride (25.0 g, 0.218 mole) and 2,6,2',6',2'',6'''-hexamethoxytriphenylcarbinol (5.0 g, 0.012 mole) were mixed in a 50 mL flask equipped with a reflux condenser, and heated in an oil bath, increasing the temperature slowly up to 205 °C in 1 h and kept at 205 °C for an additional 1 h. At the end of this time the semiliquid reaction product was poured into 150 mL of water and the solids remaining in the reaction flask were washed out with 100 mL of water. The dark orange mixture was filtered to remove an insoluble red material and was then basified in an ice-water bath with aqueous sodium hydroxide which discharged the color and produced a white precipitate. The mixture was allowed to stand at 0 °C for 1 h and the solid was collected on a filter, washed with 10 mL of water, dried, ground into powder and further dried in vacuo at 100 °C to give a white powder 0.96 g, yield 28%, mp > 200 °C, dec. (lit. 200-229 °C, dec.). UV/visible (0.1N HCl): λ_{max} ($\lg \epsilon$) = 210 (4.79), 240 (4.73), 282 (4.51), 330 (4.60), 454 nm (4.02) (br). IR(KBr) 3495 (-OH), 3070, 2860, 1618, 1488, 1460, 1277, 1270, 1202, 1070, 1020, 951, 800, 768, 750, 672, 581 cm^{-1} .

Sesquixanthryl⁺TCNQ⁻: To a suspension of sesquixanthrol (50 mg, 0.166 mmole) in 3 mL of water stirring in an ice-water bath, 2 mL of 10% aqueous

hydrochloric acid (5.4 mmole) was added dropwise which yielded a clear orange solution, to which a clear dark blue solution of Li^+TCNQ^- (35 mg, 0.166 mmole) in 2 mL of water was added dropwise in 2 min to give a precipitate. The mixture was stirred at room temperature for 3 h and the solid was collected on a filter, washed with ether and dried at 100 °C to give a dark brownish blue powder 68 mg, yield 84%, mp > 400 °C (turned dark). UV/visible (CH_3CN): λ_{max} (lg ϵ) = 232 (4.21), 278 (3.93), 325 (4.07), 390 (4.53), 478 (3.48), 676 (3.58), 741 (4.05), 756 (3.99), 838 nm (4.33). IR(KBr) 3048, 2888, 2160 ($\text{C}\equiv\text{N}$), 1628, 1540, 1508, 1416, 1336, 1118, 1066, 1023, 858, 818, 783, 740, 690, 671, 560 cm^{-1} .

Sesquixanthryl $^+$ TCNQ(N_2S) $_2^-$: To a suspension of sesquixanthrol (50 mg, 0.166 mmole) in 3 mL of water stirring in an ice-water bath, 0.5 mL of 10% aqueous hydrochloric acid (1.4 mmole) was added dropwise which yielded a clear orange solution, to which a brown solution of $\text{Li}^+\text{TCNQ}(\text{N}_2\text{S})_2^-$ (75 mg, 0.167 mmole) in 5 mL of water was added by portions to give a precipitate. The mixture was stirred at room temperature overnight and allowed to stand for 1 day. The solid was collected on a filter, washed with 3 mL of water, and dried at 100 °C to give a black powder 110 mg, yield 92%, mp 240-260 °C (dec.). UV/visible (CH_3CN): λ_{max} (lg ϵ) = 240 (4.62), 262 (4.38), 284 (4.80), 296 (5.01), 306 (4.53), 332 (4.48), 363 (4.42), 382 (4.74), 529 (3.40), 574 (3.60), 631 nm (3.84). IR(KBr) 2170 ($\text{C}\equiv\text{N}$), 1618, 1445, 1428, 1392, 1329, 1235, 1052, 1016, 839, 810, 775, 668, 500 cm^{-1} .

VI. TWO TERMINAL ORGANOMETALLIC LOGIC ELEMENTS FOR NOVEL COMPUTER ARCHITECTURE APPLICATIONS

We have evaluated the possibility of building an associative memory using organic molecular materials. We have previously reported on two-terminal bistable electrical switching and memory phenomena observed in polycrystalline films of either copper or silver complexed with the electron acceptors tetracyanoethylene (TCNE), tetracyanonaphthoquinodimethane (TNAP), tetracyanoquinodimethane (TCNQ), and various TCNQ derivatives.

The basic configuration of the logic device consists of a thin polycrystalline film of a copper or a silver charge-transfer complex sandwiched between two metal electrodes to which an electrical connection can be made. We have developed both a solution and an all solid-state technique, both compatible with microelectronic techniques, to make these two-terminal switching devices, exhibiting sharper switching characteristics, for use in large arrays.

We have been able to prepare a 2x2 matrix of 1 bit two-terminal bistable switching elements based on organic semiconducting materials grown by a solution technique, as described in previous work by our group. On a cleaned glass or sapphire substrate, ~ 1 μm thick pad of copper or silver was vacuum deposited in a line pattern. These metal lines were then reacted with TCNQ dissolved in dry acetonitrile. Thick metal-TCNQ films are known to grow in a short time period using this technique. When removed, the film was rinsed with dry acetonitrile, and as a final step of the fabrication process a second metal pad, usually aluminum, is evaporated over the polycrystalline organic semiconductor. A photograph of the matrix, is shown in Figure 1, and a photograph of a magnified two-terminal bistable switching element prepared by this technique is shown in Figure 2.

Threshold and memory behavior was observed in each of these logic elements by examining current as a function of voltage across the two-terminal structure.

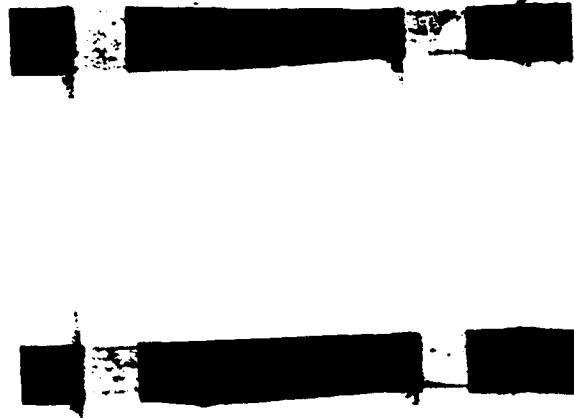


Fig. 1 Photograph of 2x2 matrix of organic switching element.

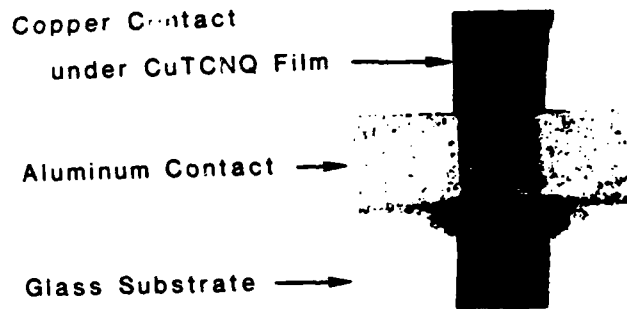


Fig. 2 Photomicrograph of AgTCNQ bistable switching element.

Figure 3 shows a representative dc current-voltage curve for a Cu/Cu-TCNQ/Al system. The trace in Figure 3 is made with a $10^2\text{-}\Omega$ load resistor in series with the device. There are two stable non-ohmic resistive states in the

material. Switching occurs when an applied potential across the sample surpasses a threshold value (V_{th}) of 9V for this array.

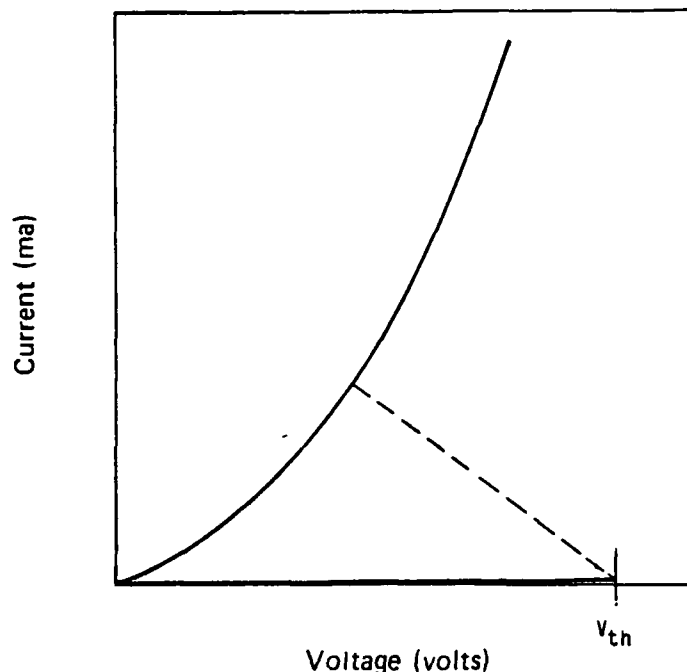


Fig. 3 Typical dc current voltage characterization showing high- and low-impedance states for a metal-TCNQ sample.

The value of V_{th} is sample dependent, ranging from 5-10 V and is proportional to film thickness. At this field strength the initial high impedance in the range of 1×10^4 ohms drops to a low impedance value of a few hundred ohms. A rise in current and decrease in the voltage along the load line (dotted line) is observed in the Cu-TCNQ system. The results in Figure 3 are representative of the switching effects observed in all of the metal charge-transfer salts examined and is characteristic of two terminal S-shaped or current-controlled negative-resistance switches.

In addition, it has been observed that once the film is in the conducting state it will remain in that state as long as an external field is applied. In every case studied, the film eventually returned to its initial high-impedance state after the applied field was removed. It was also found that the time

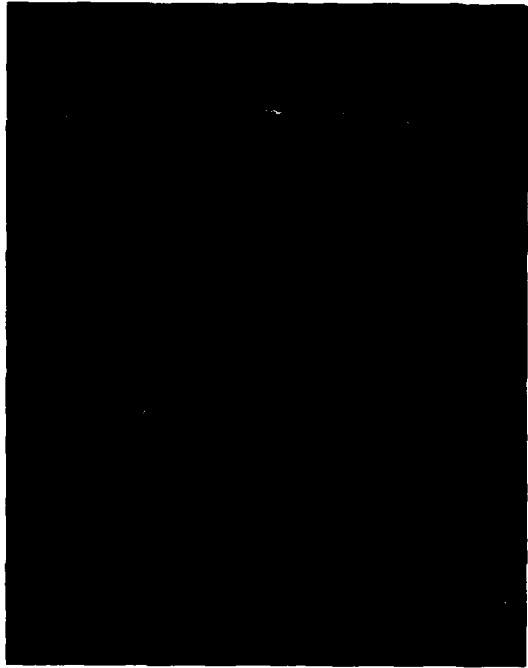
required to switch back to the initial state appeared to be directly proportional to the film thickness, duration of the applied field, and the amount of power dissipated in the sample while in the low impedance state as well as the choice of donor metal and electron acceptor species.

More recently, we have investigated a solid state technique for making these switching elements. Registered directly over a metal pad a thin film of a neutral organic acceptor species is deposited by vacuum sublimation. The two layered film on the insulating substrate is then heated to 200°C to react the metal with the organic acceptor molecule. The heat causes a rapid oxidation-reduction reaction to occur in which the corresponding metal salt of the ion radical acceptor is formed. As a consequence of the heat treatment, any unreacted neutral acceptor molecule is sublimed off of the surface of the charge-transfer complexes.

The response of one sample of this type to a single rectangular wave form pulse is shown in Figure 4. When the voltage was increased slightly above the threshold voltage, the device abruptly switched to a low-impedance state, the voltage pulse across the systems of this type before switching ranged between 5 to 10 V, depending on the thickness of the film. The sample returned to the high-impedance state rapidly upon lowering the applied potential below the threshold value.

A recent report in the literature by M. Yokoyama et al from Osaka University describes a new type of image storable organic photoreceptor for electrophotography using the electrical switching and memory phenomena that we have reported in the CuTCNQ class of materials.

The structure and mechanism for the photomemory is shown in Figures 1 and 2 of the reprint attached at the end of the section of the report (See Enclosure A).



CURRENT
(5 mA/DIV)
VOLTAGE
(5 v/DIV)

TIME (5 μ sec/DIV)



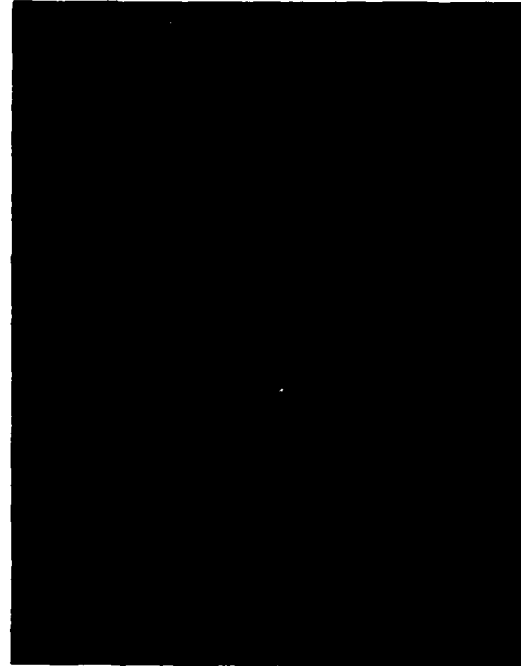
CURRENT
(5 mA/DIV)
VOLTAGE
(5 v/DIV)

TIME (5 μ sec/DIV)



CURRENT
(5 mA/DIV)
VOLTAGE
(5 v/DIV)

TIME (5 μ sec/DIV)



CURRENT
(5 mA/DIV)
VOLTAGE
(5 v/DIV)

TIME (5 μ sec/DIV)

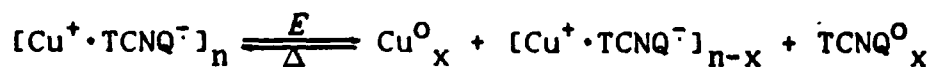
Fig. 4 Single pulse I-V characteristics for CuTCNQ solid state films.

IMAGE STORABLE ORGANIC PHOTORECEPTOR USING ELECTRICAL SWITCHING IN Cu·TCNQ COMPLEX

M. Yokoyama, Y. Kishimoto and S. Kusabayashi
Chemical Process Engineering, Faculty of Engineering,
Osaka University, Yamadaoka, Suita, Osaka, 565 Japan

The conventional electrophotography based on the Carlson method consists of the repetitions of six fundamental processes, in principle, i.e., (1) corona charging, (2) image exposure, (3) development with toner, (4) toner image transfer onto a plain paper, (5) fixing, and (6) cleaning. If the photoreceptor can memorize the first exposure image in a form of persistent conductivity, multi-duplication will be possible without every exposure in the subsequent duplication process. Many attempts have been made on such "photomemory effect" of the photoreceptors from the earlier stage. One of the examples appeared in the PVK (poly-*N*-vinylcarbazole)-TNF (2,4,7-trinitrofluorenone) organic photoreceptor adding some sort of leuco dyes or diazonium salts as reported by E. Inoue *et al.* [1].

On the other hand, R.S. Potember *et al.* recently discovered the field-induced electrical switching from high impedance "off-state" to low impedance "on-state" with the conductivity change of about 4 orders at the field strength of $\sim 10^4$ V/cm, and the memory effect of the on-state in Cu·TCNQ (tetracyanoquinodimethane) charge-transfer complex polycrystalline film grown on a Cu metal foil from TCNQ solution [2]. The switching in this complex is interpreted as a result of the formation of highly conducting complex salts involving neutral TCNQ, in other word, mixed-valence state due to the field-induced redox reaction, i.e.,



The present paper describes a new type of image storable organic photoreceptor using the switching and memory phenomena in Cu·TCNQ complex.

Structure and Basic Idea for Memory Photoreceptor

The image storable photoreceptor designed consists of a PVK - TeNF (2,4,5,7-tetranitrofluorenone) organic photoconductor (OPC) and a switching underlayer (SWL) loading Cu·TCNQ microcrystalline particles in polymer binder as shown in Fig.1. Figure 2 shows the basic idea for image storage on a memory photoreceptor. Write-in due to the usual xerographic method builds up the persistent conductivity image as the on-state of Cu·TCNQ in a thin SWL due to the field-induced switching, which is caused by the high electric field within SWL as a result of accumu-

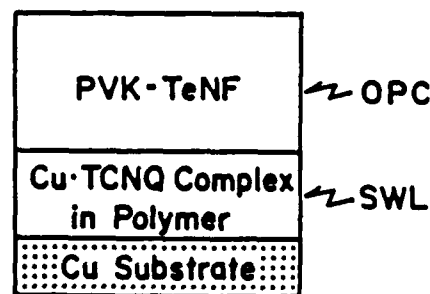
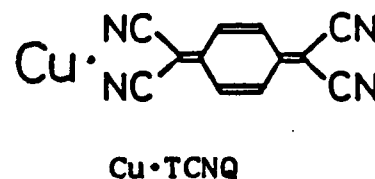


Fig.1 Structure of an image storable double layered photoreceptor.

lation of charges at the interface of OPC and SWL. For the subsequent corona charging, charge carriers injected from the bottom electrode through the highly conductive switching layer in the on-state, eliminate the surface corona charges to form the latent image on the surface of the photoreceptor.

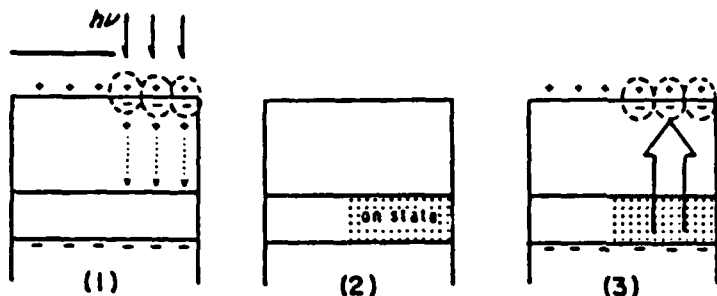


Fig.2 The basic idea for image storage on photoreceptor. (1) Corona charge and exposure (Write-in), (2) memory storage, (3) formation of latent image (Read-out).

To obtain the "photomemory" due to this mechanism, a material as an over-coating OPC is required to be transportable for the bipolar carriers as well as to be photoconductive as can be seen in the processes (1) and (3) in Fig.2. For such materials, the organic photoconducting charge-transfer complex system such as PVK-TNF is well-known. In present study, therefore, PVK-TNF or PVK-TNF charge-transfer complex systems were examined. Since Cu·TCNQ complex is an electron conductor through the well-defined column structure of TCNQ molecules, the polarity illustrated in Fig.2 is the real case.

Switching Characteristics in Cu·TCNQ Dispersion Film

Instead of Cu·TCNQ microcrystalline film grown on Cu metal foil from TCNQ solution as reported by Potember *et al.*, Cu·TCNQ dispersion films were newly examined as SWL from the viewpoints of mechanical stiffness and the practical use. The film was prepared on Cu or Al metal foil by the wired-bar coating technique from the slurry containing the ball-milled Cu·TCNQ (20 ~ 60 wt%) microcrystals and polymer resin (polyarylate resin, U-Polymer 8000, Unitika Co.) in chloroform. Film thickness was ranged from 0.5 to 2 μm .

Figure 3 shows a typical current-voltage characteristics of the Cu·TCNQ dispersion (50 wt%) film in a sandwich-typed cell with an evaporated Al electrode. Increasing the positive bias on Cu, only low current was first observed up to 2V, but beyond it (V_{th}) the current showed an abrupt increase as shown by Curve (1), indicating the switching from high to low impedance state. For the back sweep or for the repeated sweep from zero bias, the sample traced Curve (2), which showed no low current part as observed in a virgin sample (memory effect). The specific resistivities of the on (ρ_{on})

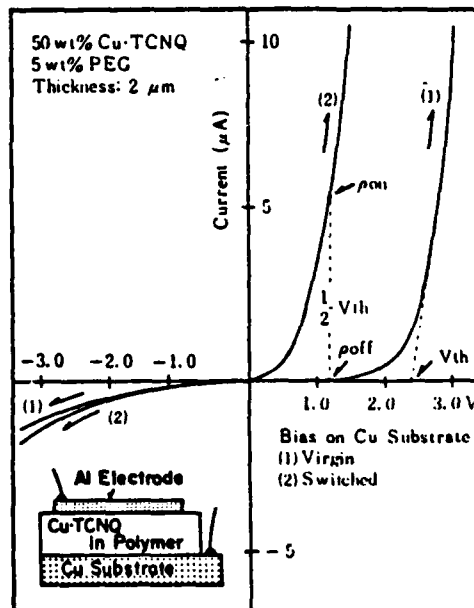


Fig.3 Typical dc current-voltage characteristics of 50 wt% Cu·TCNQ dispersion film (2 μm thick)

and off (ρ_{off}) states exhibited the difference of about 2 orders at more than 50 wt% loading of Cu·TCNQ, although fairly small as compared with the change of 4 orders in neat Cu·TCNQ polycrystalline film reported by Potember *et al.* The durability of the on-state was about 3 hours, and the heating accelerated the recovery to off-state.

Memory Effect in Layered Photoreceptor

Figure 4 shows a typical photo-memory effect of the layered photoconductor, i.e., (1) initial surface voltage (V_0) by corona charging, and (2) photodecay due to the image exposure (Write-in), and (3) surface voltage by subsequent corona charging. Fairly large charge acceptance lowering (ΔV) was obtained by the illumination, and this low charge acceptance state continued for a while. The photomemory effect is evaluated as $F_m = \Delta V/V_0 \times 100$ (%). In the case shown in Fig.4, F_m is about 60%, for example.

Figure 5 shows initial surface voltage (V_0) and photomemory ($\Delta V/V_0$) plotted against TeNF contents in the charge-transfer photoconductor. A large photomemory of ~60% was obtained near 1:0.6 mol of PVK-TeNF, while this photomemory is quite small in the PVK-TNF system and in negative charging of both PVK-TNF and PVK-TeNF systems.

In Fig.6 is shown a result indicating clearly that the charge acceptance lowering is due to the persistent conductivity formed in the photoreceptor by the xerographic write-in. The sample

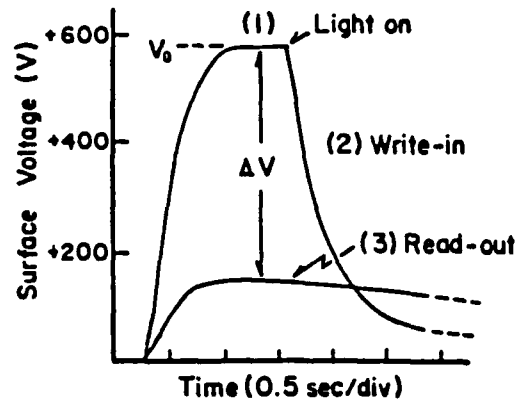


Fig.4 Typical example of photo-induced memory effect. 50wt% Cu·TCNQ, 2 μ m, PVK:TeNF=1:0.6, 7 μ m thick.

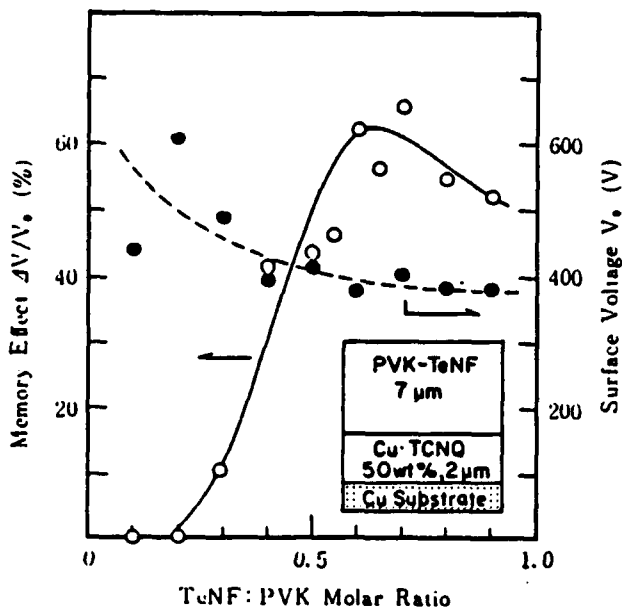


Fig.5 Dependence of initial voltage V_0 and photomemory $\Delta V/V_0$ on TeNF loading ratio in OPC.

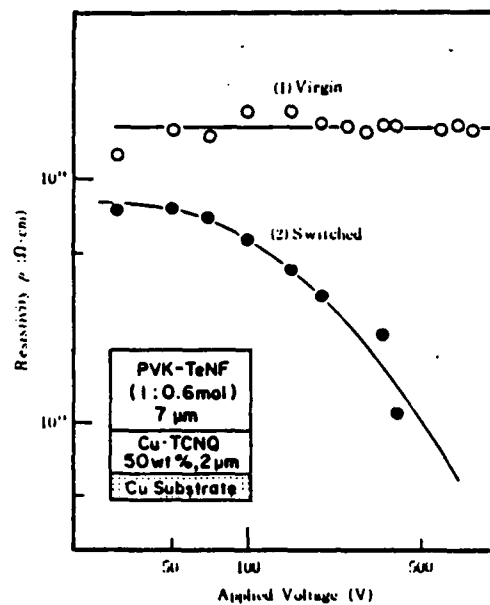
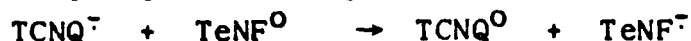


Fig.6 Specific resistivity of layered photoreceptor. (1)untreated, (2)treated.

treated with the xerographic process showed the field-dependent resistivity, while the sample without the treatment remained in almost constant resistivity of $10^{14} \Omega \cdot \text{cm}$. These results can be analyzed by the field-assisted Schottky injection of negative charge (TCNQ^-) from highly conducting switched $\text{Cu} \cdot \text{TCNQ}$ SWL to an OPC including negative-charge transportable TeNF , i.e.,



No photomemory effect in TeNF with the lower electron affinity is reasonably interpreted due to the higher barrier for the Schottky injection at the interface between SWL and OPC. Thus, TeNF^- was found to be essential for the effective photomemory.

Optimum Fabrication of Memory Photoreceptor

In Figs.7 and 8 are shown the initial surface voltage V_0 and photomemory $\Delta V/V_0$ as a function of the thickness of SWL underlayer and OPC overlayer, respectively. As an optimum fabrication, a SWL of about $2 \mu\text{m}$ loading 50 wt% $\text{Cu} \cdot \text{TCNQ}$ and an OPC of about $7 \mu\text{m}$ were obtained. The lowering of initial voltage V_0 in OPC of less than $\sim 5 \mu\text{m}$ as shown in Fig.8 is understood as due to the switching of SWL during initial corona charging process. The photomemory of more than 50% was obtained for the exposure of $\sim 1 \text{ mW}/\text{cm}^2$.

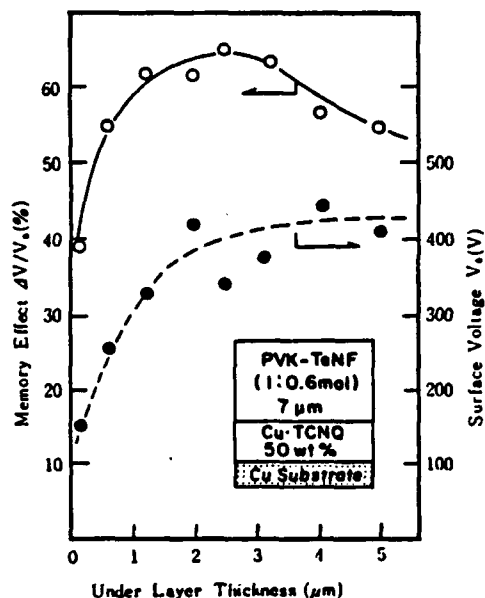


Fig.7 Photomemory $\Delta V/V_0$ as a function of the SWL thickness.

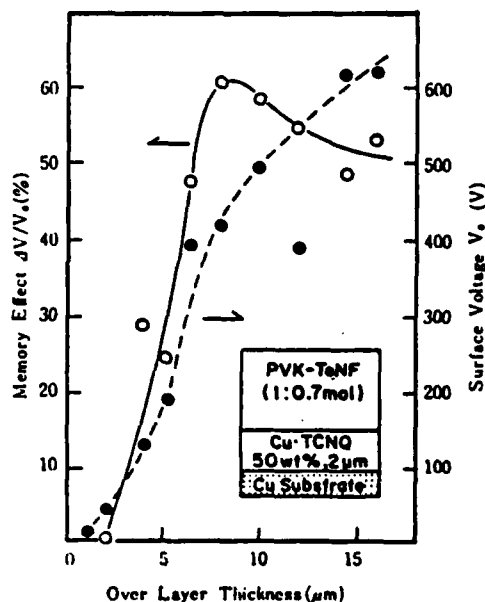


Fig.8 Photomemory $\Delta V/V_0$ as a function of the OPC thickness.

Multi-Duplication

The present image storable photoreceptor was tested as a multi-duplication master for electrostatic printing. The memory photoreceptor fabricated on Cu metal foil was corona-charged positively and exposed to a halogen lamp ($14 \text{ mW}/\text{cm}^2$, 1 min) through the image mask drawn on an OHP sheet. Then, by sticking it on a drum of a commercially available xerographic copy machine (DC-162, Mita Co.), multi-duplication of more than 50 prints was confirmed.

[1]E. Inoue, *et al.*, *Photogr.Sci.Eng.*, 22,194(1978);26,24,69(1982); 27,130(1983). [2]R.S. Potember *et al.*, *Appl.Phys.Lett.*, 34,405 (1979); *Synthetic Metals*, 4,371(1982).

VII. SOL-GEL GLASSES FOR OPTICAL INFORMATION PROCESSING MATRICES

Bistable optical switching has previously been observed in the organo metallic semiconductor compounds copper and silver tetracyanoquinodimethane (TCNQ). It has been postulated that the effect of the applied optical field on the initial charge-transfer salt (eg. AgTCNQ) is to induce a phase transition resulting in the formation of a non-stoichiometric complex salt containing neutral TCNQ. Observed changes in the optical properties of these organo-metallic materials is a direct consequence of this electric field induced reaction.

Optical switching has now been observed in colloidal AgTCNQ which has been dispersed in monolithic gel-derived silica glasses (see Figure 1). In the original synthesis of AgTCNQ described by Melby, et al, crystalline AgTCNQ powder is obtained by a metathetical reaction between AgNO_3 and LiTCNQ in water. We have now made colloidal AgTCNQ, by a modified procedure, with an average particle size of approximately 6 microns. The AgTCNQ colloid remains uniformly dispersed during the hydrolysis and polymerization of tetramethyl orthosilicate in the formation of a silicon oxide network (see Figure 7).

Our current interest centers on applications of the optical properties of these organometallic materials when exposed to either continuous or pulsed laser radiation. The two stable states of AgTCNQ have different transmission properties. When irradiated, the blue color of AgTCNQ transforms into the pale yellow color characteristic of the formation of neutral TCNQ. Transmission spectra recorded of AgTCNQ doped glass before and after this transition show significant changes in both the visible and near infrared portion of the spectrum. The large transmission changes in these organometallic containing glasses make them possible candidates for use as photochromic processors.

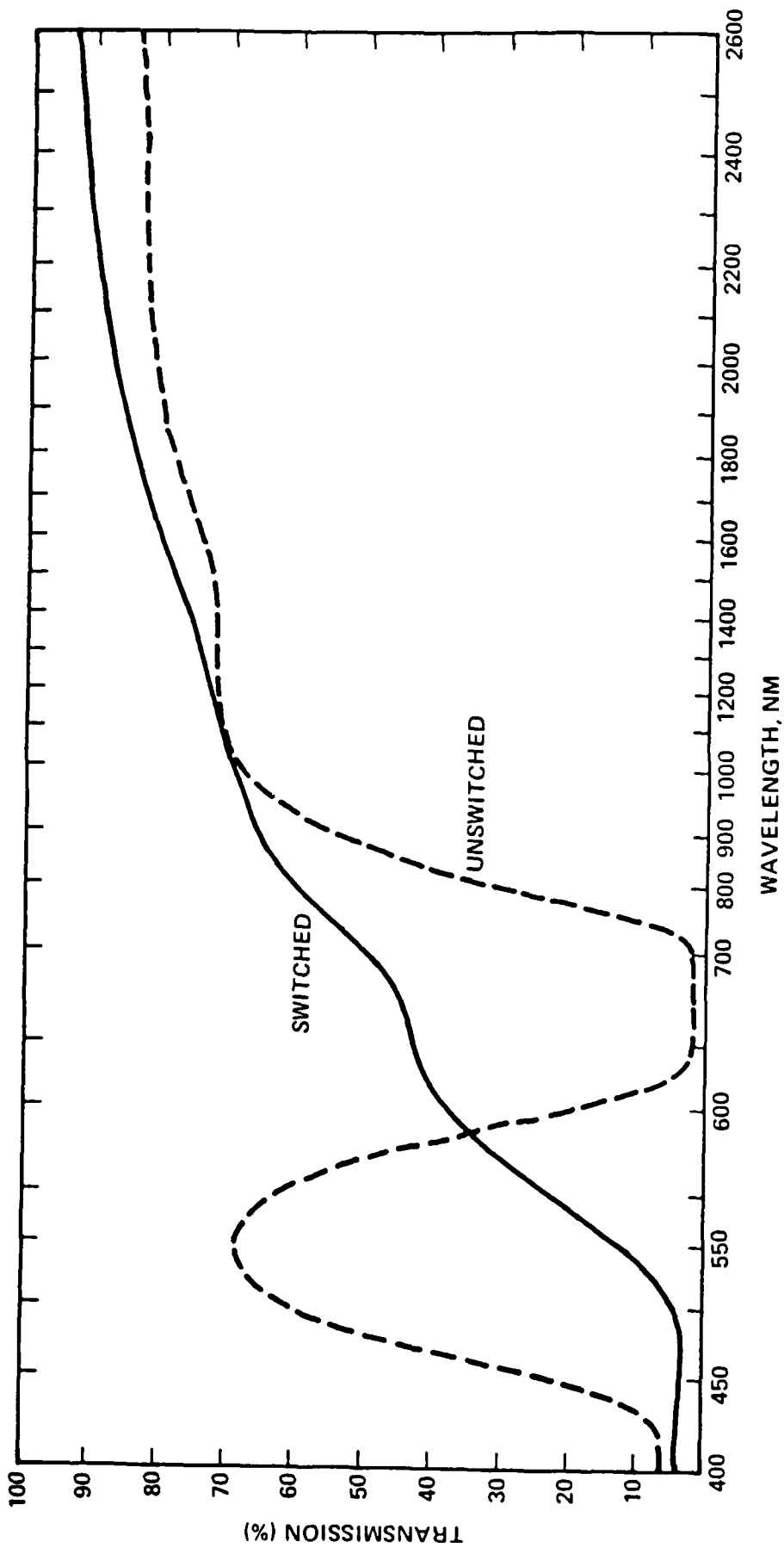


Fig. 1 Typical AgTCNQ transmission switch - 45 mJ pulses from frequency doubled Nd:YAG laser (532 nm).

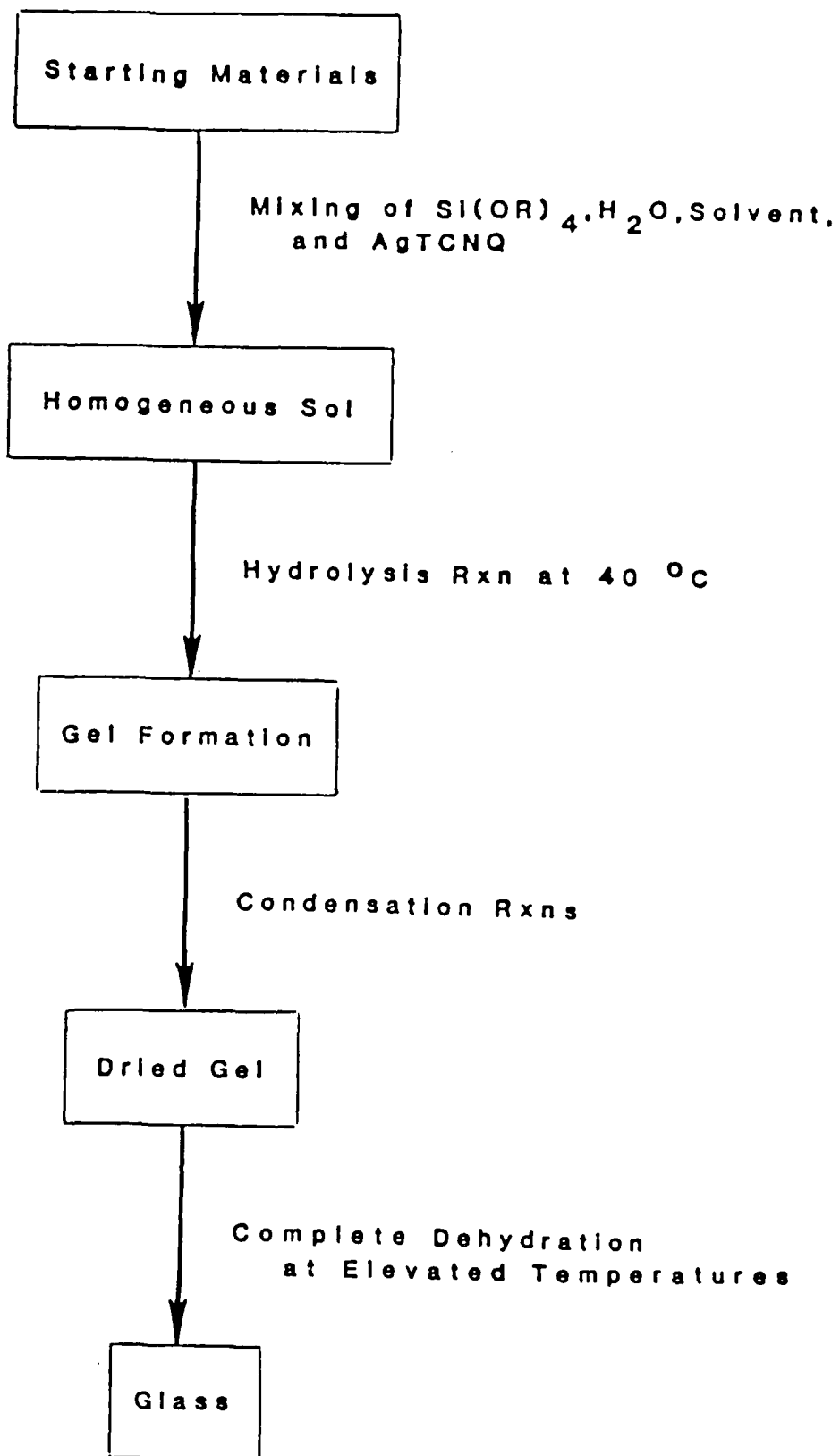


Fig. 2 Preparation of glasses by Sol-Gel Method.

VIII. VO₂ FILMS FORMED BY THE SOL-GEL PROCESS

A. Introduction

Thin films of vanadium dioxide are known to undergo a reversible thermally-induced metal-semiconductor phase transition near 67°C [1,2]. Associated with this transition, the material exhibits dramatic changes in its optical, electrical, and magnetic characteristics with respect to temperature [3,4]. This anomalous behavior has prompted considerable interest in fabricating vanadium dioxide films for both scientific investigation and for use in various technological applications [5,6].

There have also been numerous studies involving the incorporation of various dopant ions into the VO₂ lattice. It was observed that the transition temperature may be raised or lowered depending on the choice of the dopant ion. Dopants such as tungsten, molybdenum, and tantalum are known to decrease T_t with increasing concentration, with tungsten having the largest effect per atomic percent added [6-9]. In each case, the resistance ratio before and after the transformation decreases quickly for low doping levels. However, large changes in the infrared transmittance are observed even when the resistance ratio is small [7].

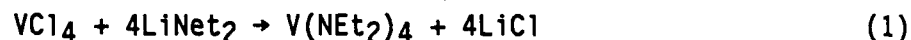
Traditionally, vanadium dioxide thin films have been prepared by either vacuum deposition [3,10,11] or chemical vapor deposition techniques [12,13]. Recently, Greenberg [7] grew vanadium dioxide thin films from vanadyl (V) triisopropoxide by gelation-hydrolysis followed by post-reduction. However, thin films of vanadium dioxide are not easy to grow by these techniques. Careful control of the deposition atmosphere is needed to maintain the proper chemical composition. Also, post-reduction of higher oxide thin films is difficult to control. The reduction process tends to leave the films inhomogeneous and porous, which degrades the switching properties of the film [7].

We report on the first doped and undoped vanadium dioxide thin films that have been prepared from an organometallic compound with an oxidation state of (IV) on the vanadium metal by the sol-gel process [14]. Formation of VO_2 from a tetravalent starting material may lead to more homogeneous films, and minimize the appearance of defects or other oxides in the final product. Spectral and resistive switching in thin films made in this manner have been demonstrated. The transition temperature of these gel-derived films is reported to be lowered by the incorporation of hexavalent dopant ions.

B. Experimental

Materials Preparation

Vanadium (IV) tetraisopropoxide, $\text{V}(\text{OC}_3\text{H}_7)_4$, was synthesized following Thomas' procedure [15,16]. This method involved a two-step reaction, as shown below



Both reactions were performed in an oxygen-free and water-free nitrogen atmosphere to prevent subsequent oxidation and hydrolysis. Care was also taken to completely dry all solvent and glassware used. The intermediate product tetrakis(diethylamino)vanadium was formed by the reaction of lithium diethylamide with vanadium-tetrachloride in dry ether. After refluxing and overnight stirring, the ether was removed and after vacuum distillation, $\text{V}(\text{Net}_2)_4$ was isolated as a green liquid.

The vanadium-tetraalkoxides was prepared by the alcoholysis of the tetrakis(diethylamino)vanadium. The $\text{V}(\text{Net}_2)_4$ was dissolved in dry benzene and frozen to -78°C in dry ice. While stirring the $\text{V}(\text{Net}_2)_4$ vigorously, dry isopropanol in benzene was added. An exothermic reaction occurred, producing a

green solution. The solution was slowly raised to room temperature and stirred overnight. Removal of the benzene, isopropanol and liberated diethylamine, under reduced pressure, left a green solid, $V(OC_3H_7)_4$. Once collected, the $V(OC_3H_7)_4$ was stored in a dry box at all times.

Razuvaev et al., [16] discovered a much easier approach for the synthesis of the tertiary butyl derivative by reacting VCl_4 with $LiOt-Bu$ in petroleum ether. We have developed a new method to prepare vanadium tetrakis(t-butoxy), $V(Ot-Bu)_4$, in a one step reaction:



Potassium tert-butoxide was chosen over the lithium equivalent on the basis of cost. The reaction was performed in a moisture-free nitrogen atmosphere to prevent subsequent oxidation and hydrolysis. Care was also taken to dry the solvent and glassware. Methylene chloride, CH_2Cl_2 , was dried over activated alumina, then distilled from calcium hydride.

Vanadium tetrachloride (13.2 g) (Atomergic) in methylene chloride (50 ml) was added dropwise to a suspension of potassium tert-butoxide (50.0 g) (Aldrich) in methylene chloride (150 ml) and stirred at $-78^\circ C$. The reaction mixture was warmed slowly to room temperature and filtered under N_2 to give a green liquid. The solvent was evaporated and the product (3.0 g) collected after vacuum distillation. The product, which was a blue liquid [$V(Ot-Bu)_4$], was stored in a dry-box.

Film preparation and characterization

Processing of the VO_2 films is shown schematically in Figure 1. Thin films of VO_2 were deposited by dipcoating a glass slide from an alcoholic solution. Approximately 200 to 300 mg of $V(Ot-Bu)_4$ were dissolved in 10 ml of dry t-butyl

alcohol. The dry t-butyl alcohol was distilled from calcium hydride. It was also found that dry isopropyl alcohol could be used as a substitute solvent without any apparent change in the deposition parameters.

Dopant atoms were placed into the crystal structure of VO_2 by combining solutions of the vanadium alkoxide with those of tungsten or molybdenum(VI) tetrachloride oxide (Alfa). Tungsten and molybdenum were chosen as dopants because of the very large effects they have on the transition temperature. For example, MoOCl_4 (11 g) was dissolved in chosen solvent (10 ml). The solution (2.7 ml) was then added to a solution (10 ml) of $\text{V}(\text{Ot-Bu})_4$ (200 mg). The hydrolysis of the vanadium compound was catalyzed by the by-product HCl .

Corning 7059 barium borosilicate glass slides were withdrawn from the solution in nitrogen at a constant rate. A typical withdraw rate was 1 mm/sec, and was controlled using a variable speed motor. Both sides of the slide were coated using this technique. An olive-green film immediately formed on the slide when it was withdrawn from the sol. Slides were often coated more than one time to produce the appropriate thickness. To convert the films into VO_2 , they were annealed at 600°C for 30 min under N_2 to achieve complete dehydration, residual solvent removal, and crystallization.

The electrical and optical properties of these gel-derived VO_2 films were measured when heated through the transition temperature. The experimental set-up was the same as previously described [17,18]. The arrangement allowed for the concurrent measurement of electrical resistance and optical transmission at 2400 nm as a function of temperature. The data was collected and recorded by an Apple II computer interfaced to the experimental set-up. Spectral transmission of these films was also scanned above and below the transition temperature. The scan range was between 400 to 2600 nm. A Sloan Dektak was used to determine the film thickness. It was necessary to etch a sharp step to measure the film

thickness. Samples were masked with wax, then etched with dilute nitric acid. The wax was then removed with hot hexanes.

RESULTS

The electrical switching behavior of a 250 Å thick VO_2 film is shown in Figure 2. Electrical resistance decreased by one to two orders of magnitude at a switching temperature of 68°C. The resistive ratio and switching temperature observed is typical for VO_2 thin films prepared on unprimed glass by other techniques [19]. Switching occurred over a narrow range of temperatures, with sharp heating-cooling hysteresis of about 10°C. The near-IR transmittance of the film at 2400 nm, measured simultaneously with resistance, is plotted in Figure 2b. As expected, there is an abrupt decrease in transmission near 68°C.

The optical transmission of a $\text{V}_{0.98}\text{Mo}_{0.02}\text{O}_2$ film at 2400 nm versus temperature is shown in Figure 3a. It was assumed that the concentration of the dopant in the film is the same as that in solution. The transition temperature, taken as the inflection point of the heating curve, is near 56°C. The film thickness was 250 Å. Resistance changes are minimal, and therefore are not included here.

The results obtained for a $\text{V}_{0.99}\text{W}_{0.01}\text{O}_2$ are shown in Figure 3b. The thickness of the tungsten doped film was 500 Å. Switching occurred over a larger range of temperatures, but was depressed significantly lower than the undoped or molybdenum doped films. The results were similar to other work involving doped.

The switched and unswitched transmission spectra shown in Figure 4 are typical for the doped gel-derived films. Although the dopant ions greatly influence the transition temperature, they do not effect the observed spectral transmission of the film far from that for undoped VO_2 [3,7].

CONCLUSION

Doped and undoped vanadium dioxide films were deposited on glass slides from an alcoholic solution of vanadium tetrakis(t-butoxide) by

dipcoating. A new methodology was discovered in the the synthesis of the vanadium precursor. The electrical and optical behavior of these gel-derived films proved to be comparable to that observed other thin film deposition techniques.

The sol-gel process provides a versatile way of making doped VO₂-based devices. Doping is achieved by mixing metal oxychlorides or alkoxides with the vanadium precursor in solution. This technique permits mixing of the constituents at the molecular level, which leads to a more homogeneous product. The starting materials were purified by standard chemical procedures which improved the quality of the final product. It has been demonstrated that the addition of molybdenum and tungsten depresses the switching temperature with increasing concentration.

REFERENCES

1. F. J. Morin, Phys. Rev. Lett., 3 (1959) 34.
2. D. Adler, Rev. Mod. Phys., 40 (1968) 714.
3. H. W. Verleur, A. S. Barker, Jr., and C. N. Berlund, Phys. Rev. Lett., 172 (1968) 788.
4. C. N. Berglund and H. J. Guggenheim, Phys. Rev., 185 (1969) 1022.
5. F. A. Chudnovskii, Sov. Phys. Tech. Phys., 20 (1976) 999.
6. G. V. Jorgenson and J. C. Lee, Solar Energy Materials, 14 (1986) 205.
7. C. B. Greenberg, Thin Solid Films, 110 (1983) 73.
8. J. B. MacChesney and H. J. Guggenheim, J. Phys. Chem. Solids, 30 (1969) 225.
9. J. B. Goodenough, J. Solid State Chem., 3 (1971) 490.
10. C. H. Griffiths and H. K. Eastwood, J. Appl. Phys., 45 (1974) 2201.

11. M. Fukuma, S. Zembutsu, and S. Miyazawa, *Appl. Opt.*, 22 (1983) 265.
12. L. A. Rayabova, I. A. Serbinov, and A. S. Darevsky, *J. Electrochem. Soc.*, 119 (1972) 427.
13. J. B. MacChesney, J. F. Potter, and H. J. Guggenheim, *J. Electrochem. Soc.*, 115 (1968) 52.
14. R. S. Potember, K. R. Speck, and H. S-W. Hu, U.S. Patent Disclosure, 1987.
15. D. C. Bradley and M. L. Mehta, *Can. J. Chem.*, 40 (1962) 1183.
16. G. A. Ruzuvaev, V. N. Latyaeva, V. V. Drobotenko, A.N. Linyova, L. I. Vishinskaya, and V. K. Ckerkasov, *J. Organometallic Chem.*, 131, (1977), 43.
17. T. E. Phillips, R. A. Murphy, and T. O. Poehler, *Mat. Res. Bull.*, 22 (1987) 1113.
18. K. R. Speck, H. S-W. Hu, M. E. Sherwin, and R. S. Potember, to be published.
19. G. A. Rozgonyi and D. H. Hensler, *J. Vac. Sci. Tech.*, 5 (1968) 194.

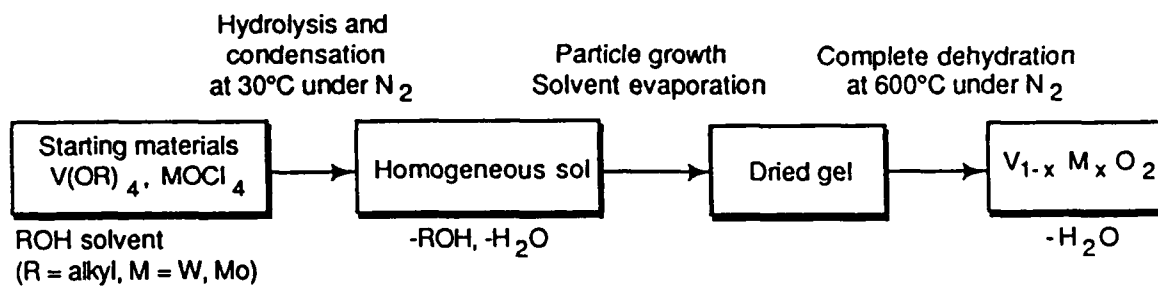


Fig. 1 Preparation of $V_{1-x}M_xO_2$ thin films by the sol-gel method.

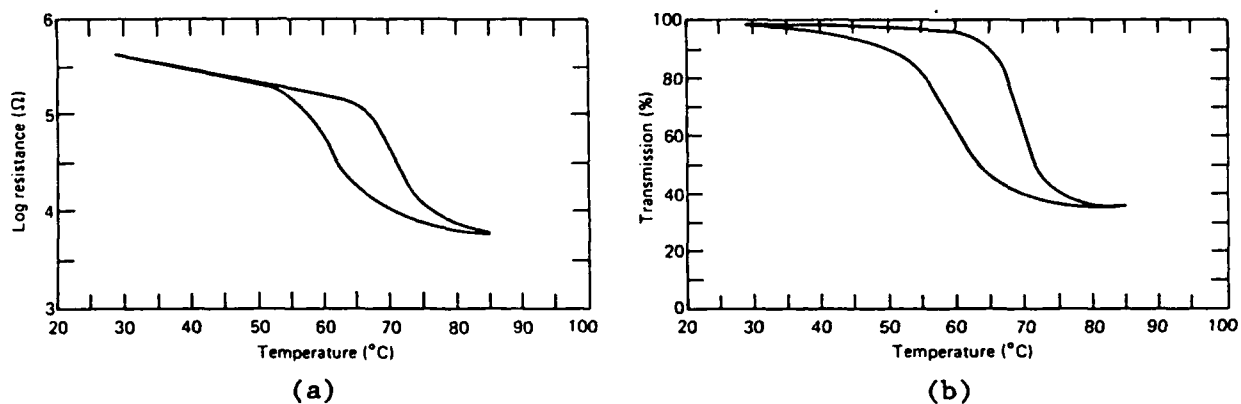


Fig. 2 (a) Temperature dependence of electrical resistance and of (b) optical transmittance at 2400 nm for a 250 Å thick film.

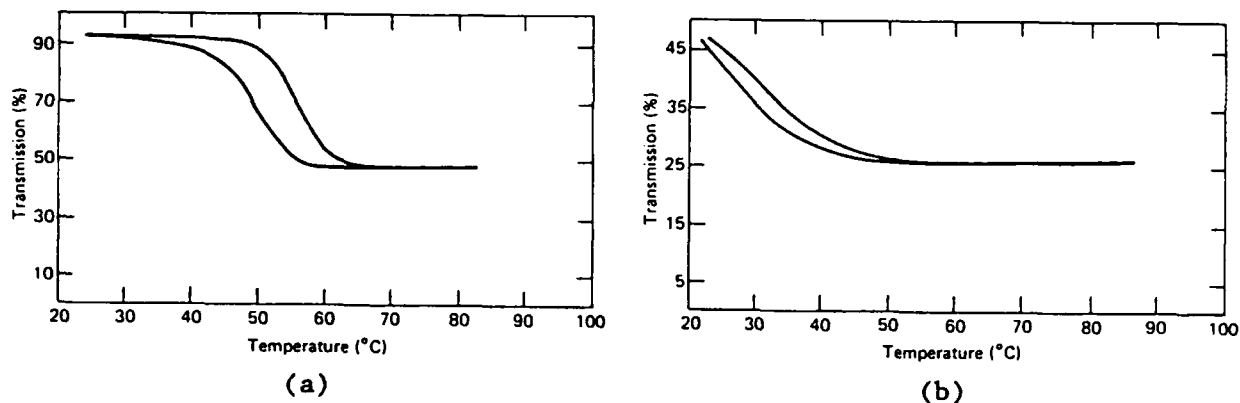


Fig. 3 (a) Temperature dependence of the transmission at 2400 nm for 250 Å thick $V_{0.98}Mo_{0.02}O_2$ film and for (b) 500 Å thick $V_{0.99}W_{0.01}O_2$ film.

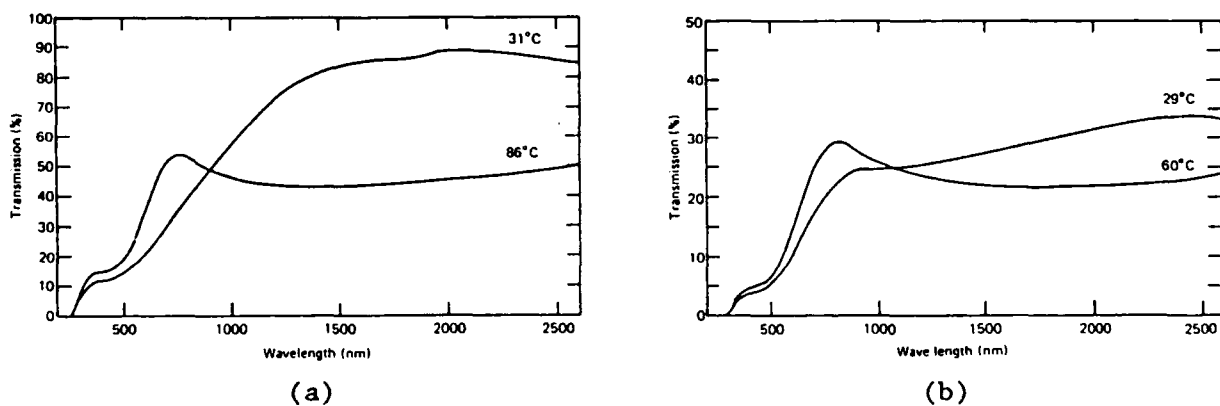


Fig. 4 (a) Spectral transmission for a 250 Å thick $V_{0.98}Mo_{0.02}O_2$ film, and for (b) a 500 Å thick $V_{0.99}W_{0.01}O_2$ film above and below the transition temperature.